E82-10064
CR-165086

EVALUATION OF HCMM SATELLITE DATA FOR ESTUARINE TIDAL CIRCULATION PATTERNS AND THERMAL INERTIA SOIL MOISTURE MEASUREMENTS

Donald R. Wiesnet — Principal Investigator
David F. McGinnis, Jr. — Co-Investigator
Michael Matson — Associate
John A. Pritchard — Associate

(E82-10064) EVALUATION OF HCMM SATELLITE DATA FOR ESTUARINE TIDAL CIRCULATION PATTERNS AND THERMAL INERTIA SOIL MOISTURE MEASUREMENTS Final Report (National Oceanic and Atmospheric Administration) 79 p
N82-20587
HC A05/MF A01
G3/43
Unclas
00064

National Oceanic and Atmospheric Administration
National Earth Satellite Service
Earth Sciences Laboratory, Land Sciences Branch
Washington, D.C. 20233

June 1981

FINAL REPORT

Prepared for: GODDARD SPACE FLIGHT CENTER
GREENBELT, MARYLAND 20771

TABLE OF CONTENTS

TABLE OF CONTENTS (cont'd)

LIST OF ILLUSTRATIONS

LIST OF TABLES

PREFACE

This report was prepared under the sponsorship of a grant to the National Oceanic and Atmospheric Administration/National Earth Satellite Service (Investigation No. HCM 045, Contract No.S-40229-B). It is prepared in three sections: Part A, pertaining to tidal circulation patterns in estuaries; Part B, pertaining to soil moisture; and Part C, pertaining to urban heat islands. Appendix A pertains to the effects of powerplant waste-water emissions on lake temperatures. Another area of investigation considered in the original proposal dealt with snowpack properties. Unfortunately no aircraft data were obtained to provide Dr. Arthur Eschner of the State University of New York/Syracuse the necessary information required for his snow study of the Cranberry Lake region in the Adirondack Mountains. Part C and Appendix A were not in the original proposal but have been added to provide further examples of useful applications of HCMR data. The purpose of this report is to evaluate the ability to extract useful information from the HCMM (Heat Capacity Mapping Mission) satellite's HCMR (Heat Capacity Mapping Radiometer) data.

The authorship of this report is a team effort, but nevertheless certain sections are primarily authored by individuals. Part A was written by Wiesnet, Part B by McGinnis and Part C by Matson. Please note that references are found at the end of each section for the readers' convenience.

ACKNOWLEDGEMENTS

Ms. Jane A. D'Aguanno provided necessary drafting talent required for many of the illustrations as well as a thorough critical review of the manuscript. Scott Staggs reduced the ground data, then prepared the illustrations for the 13 June 1979 Luverne soil moisture survey. Craig Berg prepared the

soil moisture survey flight lines map. David G. Forsyth has been involved in the computer processing as well as a myriad of other details. We acknowledge with thanks, Dr. Thomas R. Carroll of the National Weather Service, River Forecast Center, Minneapolis for providing the gamma-ray information collected on 13 June 1979, at our Luverne test site; Ms. Virginia P. Carter of the U.S. Geological Survey for the temperature data of the Potomac River; and Dr. Alden P. Colvocoresses of the U.S. Geological Survey for his analysis of HCMR data of Lake Anna. Lastly, we acknowledge the painstaking work of Mrs. Olivia Smith, and Mrs. Cathy Hall without whose expert typing and patience the report could not have been completed.

EXECUTIVE SUMMARY

CONCLUSIONS

Part A. Tidal Circulation Patterns

1. Digital thermal maps of the Potomac River estuary and the Cooper River estuary were prepared from HCMM HCMR tapes.

2. Tidal phase (flood or ebb) was correctly interpreted from gray scale thermal images and digital printouts and was later verified by tidal records.

3. Synoptic surface circulation patterns have been charted by locating thermal fronts and water-mass boundaries within the estuaries.

4. Thermal anomalies were detected adjacent to a conventional power plant on the Potomac as well as near certain communities along the Potomac.

5. Under optimum conditions, estuaries as small as the Cooper River (i.e., approximately 100km^2) can be monitored for generalized tidal/thermal circulation patterns by HCMM-type IR Sensors.

Part B. Soil Moisture

1. Computer programs were developed to enlarge and enhance HCMR data. Imagery may be produced at scales of 1:5,000,000; 1:4,000,000; 1:2,500,000; 1:1,000,000; and 1:500,000. The data are also available in character printout at the same scales as well as 1:250,000.

2. Digital thermal maps of the Luverne test site were prepared from HCMM HCMR tapes.

3. The HCMM thermal inertia approach to soil moisture estimation is unsatisfactory as a NESS operational satellite technique for temperate regions such as Luverne (in the Corn Belt) because of the high incidence of interferring cloud cover. However, the approach may well be suitable in semiarid regions such as the Southwest.

4. Because the thermal inertia technique for estimating soil moisture as exemplified by the HCMM experiment is unsatisfactory, in our view, as an operational system, we would recommend an all-weather system such as passive or active microwave for NESS if it required a soil-moisture sensor.

Part C. Urban Heat Island

1. HCMM HCMR thermal-IR data reveal similar structure of the Baltimore and Washington heat islands when compared to NOAA AVHRR thermal-IR data.

2. Small suburban and industrial areas can also be identified on each image.

Appendix A. Nuclear Power Plant Waste Water

1. Thermal anomalies resulting from warm discharge water of a nuclear power plant were mapped in Lake Anna (52.6sq. km), Va.

PART A: TIDAL CURRENT CIRCULATION PATTERNS IN ESTUARIES

INTRODUCTION

Increased awareness of the ecological importance of estuaries in terms of marine life, public health, and coastal pollution problems has led government officials and environmentalists to seek improved techniques for monitoring the fragile estuarine ecosystems of our coastal zone. With the belief that the high spatial and thermal resolution of the HCMM satellite could perhaps contribute to the monitoring of the surface current patterns in estuaries, several test sites were selected for study. Previous studies of estuarine circulation dynamics, primarily by aircraft thermal imagery, had been successful (Wiesnet and Cotton, 1967; Hartwell, 1970; and Wiesnet, 1972). Further, in 1973, Mairs and Clark (1973) used thermal-IR in conjunction with dye studies and aircraft sequential photography to measure the movement of water fronts and to prepare streamline analysis charts of circulation for the Patuxent River estuary in Maryland.

Launched in 1972, both the NOAA-2 and Landsat-1 satellites were instrumental in profoundly changing our approach to observing water bodies. NOAA-2's VHRR was capable of revealing details of large scale ocean current dynamics through the use of its thermal channel. In fact, the charting of the Gulf Stream soon became an operational task of NOAA/NESS oceanographers, who were able to include phenomena previously seldom observed and poorly understood, e.g., cold and warm eddy motion. Landsat-1, which collected little data over the open ocean, nevertheless collected copious quantities of multispectral data over U.S. coastal regions. Klemas (1974) reported on his findings from multispectral analysis of images of Delaware Bay. By using turbidity as a tracer and other techniques he was able to demonstrate clearly that one can observe a

variety of current indicators from the visible band data and that a synoptic current chart could be derived from these interpretations. Klemas (1980) in a subsequent paper was able to use Landsat data to identify fronts, which materially affect oil-slick movement, and incorporate these frontal locations into an oil drift and dispersion model thus to improve the model's performance.

But the advent of HCMM in April 1978, provided a potentially better tool for monitoring estuarine circulation patters. HCMM was better because it permitted both nighttime observations, and more frequent observations. It provided the best thermal resolution (0.5°C) combined with the best spatial resolution (600 m) thus far available from any NOAA or NASA unmanned satellite.[1/]

CURRENTS

Currents are commonly classified as tidal and nontidal, but in reality all local currents are a combination of both tidal and nontidal forces. The currents described in this study are primarily tidal and arise from astronomically produced tidal changes of water level. Meteorological factors, especially wind, can cause significant changes in both water levels and currents.

Tidal currents may be further subdivided into rotary or reversing. Tidal currents in rivers and straits are reversing as their confinement changes the resolution of forces from rotational to an upriver/downriver situation, known in nautical parlance as flood or ebb currents. In this report, our concern is with these rather dynamic reversing currents and their changing distribution throughout the tidal cycle.

Reversing tidal current cycles may be thought of as "beginning" at high slack water, and as passing through several phases, viz.:

1. high slack water
2. ebb flow
3. low slack water
4. flood flow

1/ The Landsat-3 thermal band (Price, 1980) had a spatial resolution of 250 m but poor thermal resolution. It was never fully operational.

Obviously, there is a gradual transition from phase to phase with accompanying gradual changes in current speeds and current directions.

Chesapeake Bay and its tributaries represent moderately stratified estuaries as does the estuarine portion of the Delaware River--but not the wider portion of Delaware Bay--and the harbor of Charleston, South Carolina.

In the moderately stratified estuary, the dominant mixing agent is turbulence caused by tidal action rather than velocity shear at the interface between the salt water and the overlying freshwater layer (Pritchard, 1967).

DELAWARE BAY

Although our HCMM test sites do not include Delaware Bay, we did receive a very fine cloud-free image of Delaware Bay in 1979. The image was an 11 June 1978 nighttime IR image. Using programs developed by John Pritchard of NESS, especially for HCMM CCT data, an enhanced 1:1,000,000 image was prepared at NOAA/NESS using the Digital Muirhead Device (DMD) (Fig. 1).

Although not a NESS/HCMM test site, we wanted to test our thesis that the thermal patterns in an estuary could be used to determine the tidal current circulation patterns from satellite IR imagery. The interpretation of the pattern shown in the Delaware Bay estuary clearly shows cool sea water invading the estuary. The warmer upland (fresh) water is restricted to the upper portions of the bay. A mid- or early-flood situation was estimated in the lower bay. Fig. 2 is a chart prepared from NOAA tidal current charts that shows, by means of arrows, the current as determined by current meters, two hours before maximum flood at the Bay entrance. The chart appears to be in correspondence with the surface truth and circulation patterns as interpreted from HCMM data.

POTOMAC RIVER ESTUARY

The Potomac River is an estuary in its lower portion from the Chesapeake Bay upstream to Washington, D.C. Tidal effects are detectable all

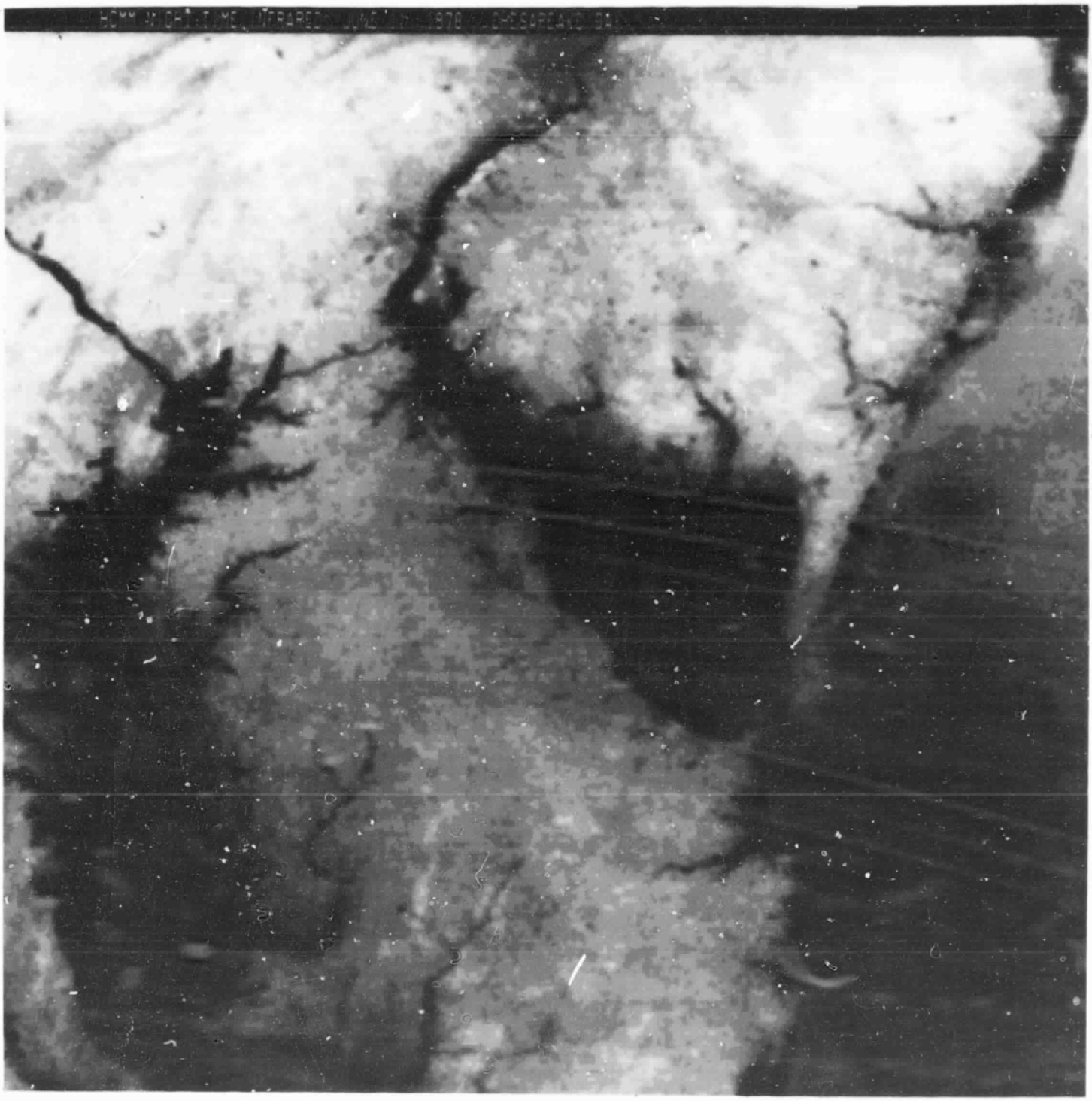

Figure 1. HCMM thermal image of 11 June 1978 (1430 hours local) of the Delaware Bay estuary. The cold (light-toned) Atlantic marine water is flowing into the Bay at the onset of a flood tide. Upriver, the Delaware is still at ebb flow.

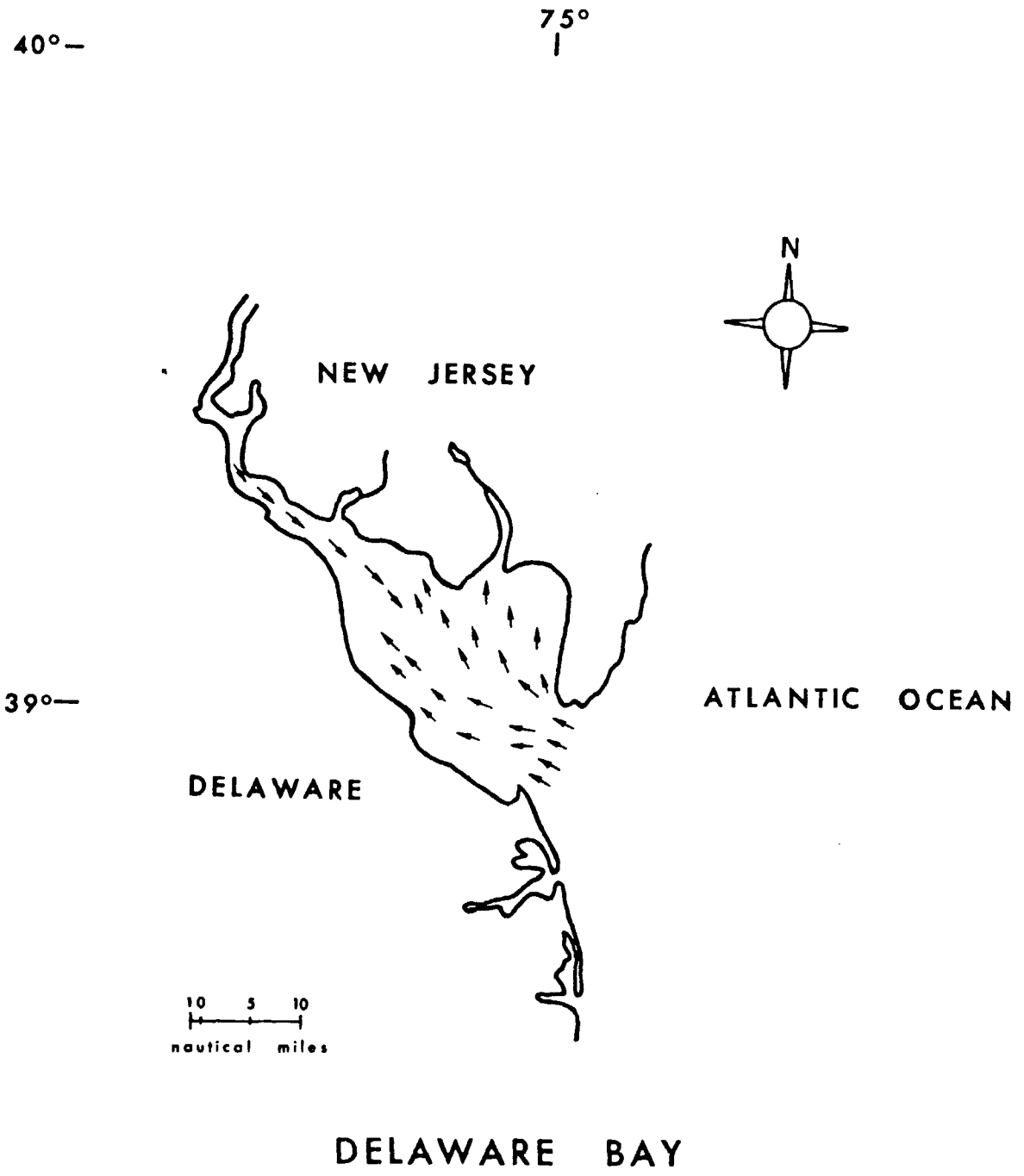

Figure 2. This sketch map of the Delaware Bay was taken from National Ocean Survey Charts based on current measurements two hours before maximum flood. Compare with Figure 1.

the way to Great Falls, but our study will concern itself only with the lowermost Potomac (see Fig. 3) as only this portion is wide enough to be easily detected by HCMM. A sequence of images on 16-17 March 1979, has been selected to demonstrate how thermal data may be used to detect estuarine circulation patterns from satellites with high thermal sensitivity (i.e., able to detect Δt's as small as 0.5°C) and moderately good spatial resolution (i.e., as high as 1 km). The following three images will be analyzed:

1.	HCMM HCMR Daytime IR	1855Z	16 March 79 (Fig. 4)
2.	TIROS-N AVHRR Daytime IR	1959Z	16 March 79 (Fig. 5)
3.	HCMM HCMR Daytime IR	1813Z	17 March 79 (Fig. 6)

These essentially cloud-free images were selected from hundreds of HCMM images examined. As may be expected, cloudiness is a considerable problem in satellite thermal-IR studies, especially in the temperate zone. In fact, it renders this technique ineffective as an operational scheme. Nevertheless, as will be pointed out, a considerable amount of information may be deduced from careful analysis of the imagery, and the information may be applied to estuaries that are insufficiently studied for a better understanding of the dynamics of circulation under varying conditions.

The 1355 (1855Z) local time HCMM image of 16 March 1979

In this image (Fig. 4) dark is hot; white is cold. Note the rather uniform temperature of Chesapeake Bay. Although a few patches of sea water (coldest) are afloat in the bay, the temperature of both the Potomac--downriver from Coles Point--and the bay are identical. From Coles Point upriver the temperature is also very uniform, but warmer. This simple straightforward condition is interpreted as an example of the sea water (Chesapeake Bay water will be referred to as sea water) moving upriver on a rising tide. The currents are flooding, moving upstream, in the sea water portion of the estuary. The

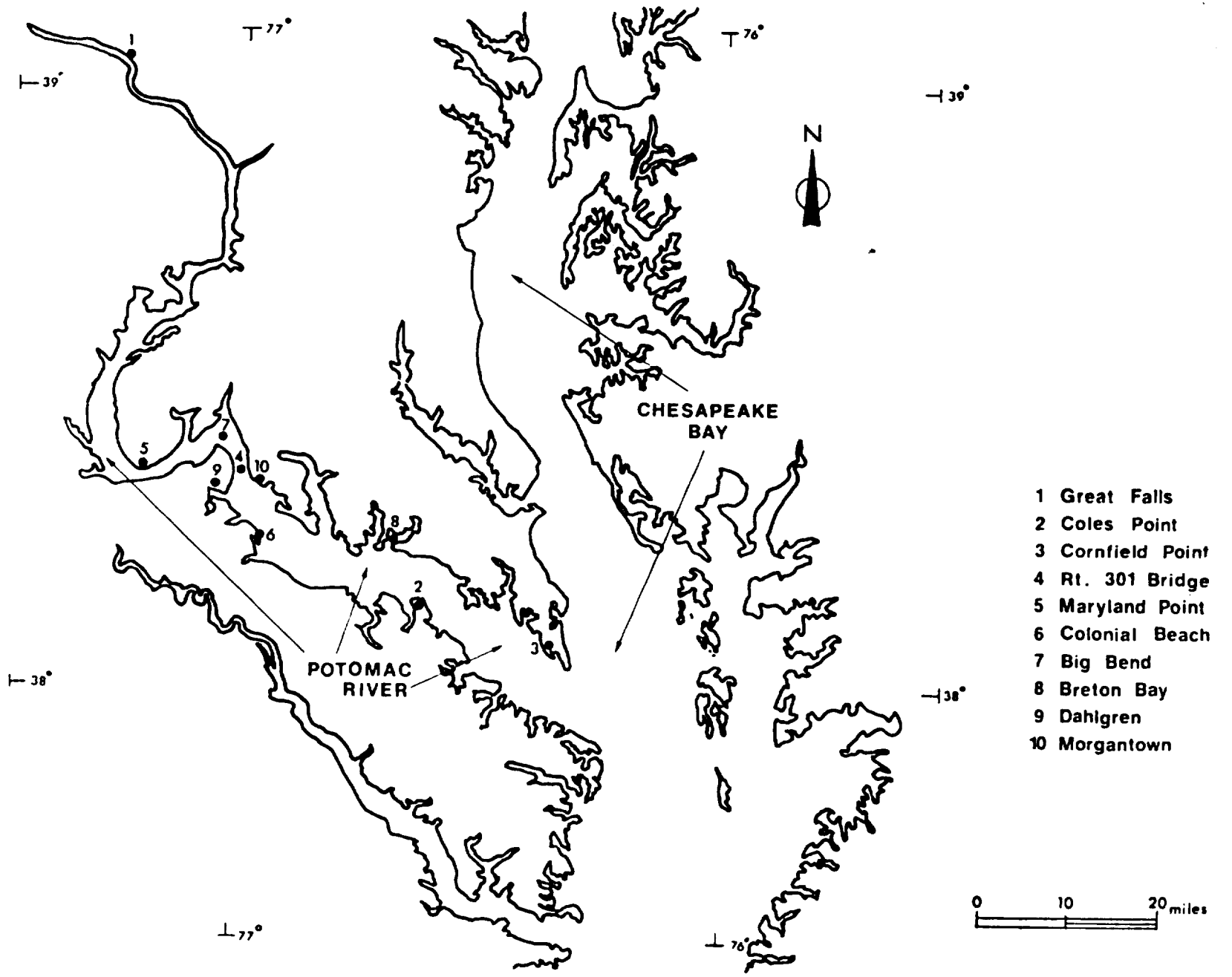

Figure 3. Index map of the Potomac River test site showing localities mentioned in the report.

Figure 4. HCMM daytime thermal image of 16 March 1979 (1755Z) (1255 local time) of the Potomac River estuary. Dark areas are cold; white areas are hot. The estuary is in mid-flood stage. The change in tone indicates the approximate position of the tidal "front".

abrupt temperature change delineates the approximate position of the tidal front (Fig. 4).

This interpretation of the thermal image is in agreement with the predicted tidal levels and currents (NOAA, 1979). In mid-channel off Cornfield Pt. flood currents are approaching maximum flood velocity, in excess of 0.4 knots, a condition that will exist in 19 minutes, at 1416. Upstream at the Potomac River Bridge (Rte. 301) (Fig.4) currents are decreasing and slack low water will occur in one hour at 1455. Upstream at Maryland Point, ebb currents reached their maximum about 2 hours earlier (1140). In summary, as the flooding cooler sea water moves upriver, slack water (warmer) precedes it and upriver ebb currents become increasingly weak.

The 1459 local time (1959Z) AVHRR image of 16 March 1979

We secured a tape of the TIROS-N AVHRR pass over the Potomac River that occurred about two hours later than the HCMM image. The thermal patterns had changed. At the mouth of the river the image (Fig. 5) reveals a temperature change between the colder bay water and the warmer river water. A flooding situation is still in progress with water levels rising in the lower Potomac estuary, and this situation will pertain for several hours. But upstream at the U.S. Route 301 Potomac River Bridge, slack water is occurring. At Colonial Beach, high tide is about an hour away, but in the main channel, currents as far upriver as Maryland Point are entering the high water slack that will be followed by the onrushing ebb as the river discharge gradually overcomes the tidal forces. The water is warm in the narrow reach of the river at Maryland Point; it is cooler at Big Bend; it is warmer again as it passes under the U.S. Route 301 Bridge. It is believed (lacking appropriate ground truth) that the water off Maryland Point is warmed by the slack water change, i.e., turbulence is greatly reduced during this interval. Turbulent flow brings up cooler water from depth. The tidal front is thus judged to be just downstream. The warming

Figure 5. AVHRR daytime thermal image of 16 March 1979 (1959Z) (1459 local time). This NOAA TIROS-N image was taken two hours after Figure 4. Mid-flood conditions pertain, but high water slack is occurring off Maryland Point where the water appears slightly warmer owing to a lessening turbulent flow.

that takes place in the U.S. Route 301 Bridge area is believed due to the spreading of the warm water discharge of the power plant at Morgantown. Ordinarily during times of turbulent flow this warm effluent is quickly mixed vertically. At times of slack water or weak current it can spread more extensively over the surface. The slightly warmer water from Morgantown to Breton Bay appears to be the result of this discharge. This interpretation was not verified by ground truth.

The 1313 local time (1813Z) HCMM image of 17 March 1979

The third image (Fig. 6) is perhaps the most interesting of the three. As in the previous day's HCMM image, the temeprature of the sea water and lower river water are identical. Along the north side of the estuary above Breton Bay and opposite Colonial Beach, the sea water has penetrated farther than along the south shore. During flood flows (looking upstream), this right-hand movement of the sea water is characteristic of Northern Hemisphere estuaries and it is caused by the coriolis force.

Dynamically, currents are flooding in the main channel at the river mouth and are increasing in strength. At the Potomac River U.S. Route 301 Bridge the ebb currents are diminishing from their peak an hour earlier at 1216. The same is true of the main channel at Maryland Point where maximum flood occurred at 1231--42 minutes prior to the overpass. It is interesting, but hardly unexpected, to note that the thermal patterns in the Patuxent and Rappahannock are quite similar. Both their tidal cycles are likewise quite similar to that of the Potomac River.

Just off the Potomac River mouth is a large mass of warm water almost bifurcated by cooler bay water. The same thermal phenomenon occurs off the mouth of the Rappahannock. In our view these water masses represent the prior cycles' discharge of upland river water expended into the bay for eventual assimilation. Again these observations are speculative, but similar features

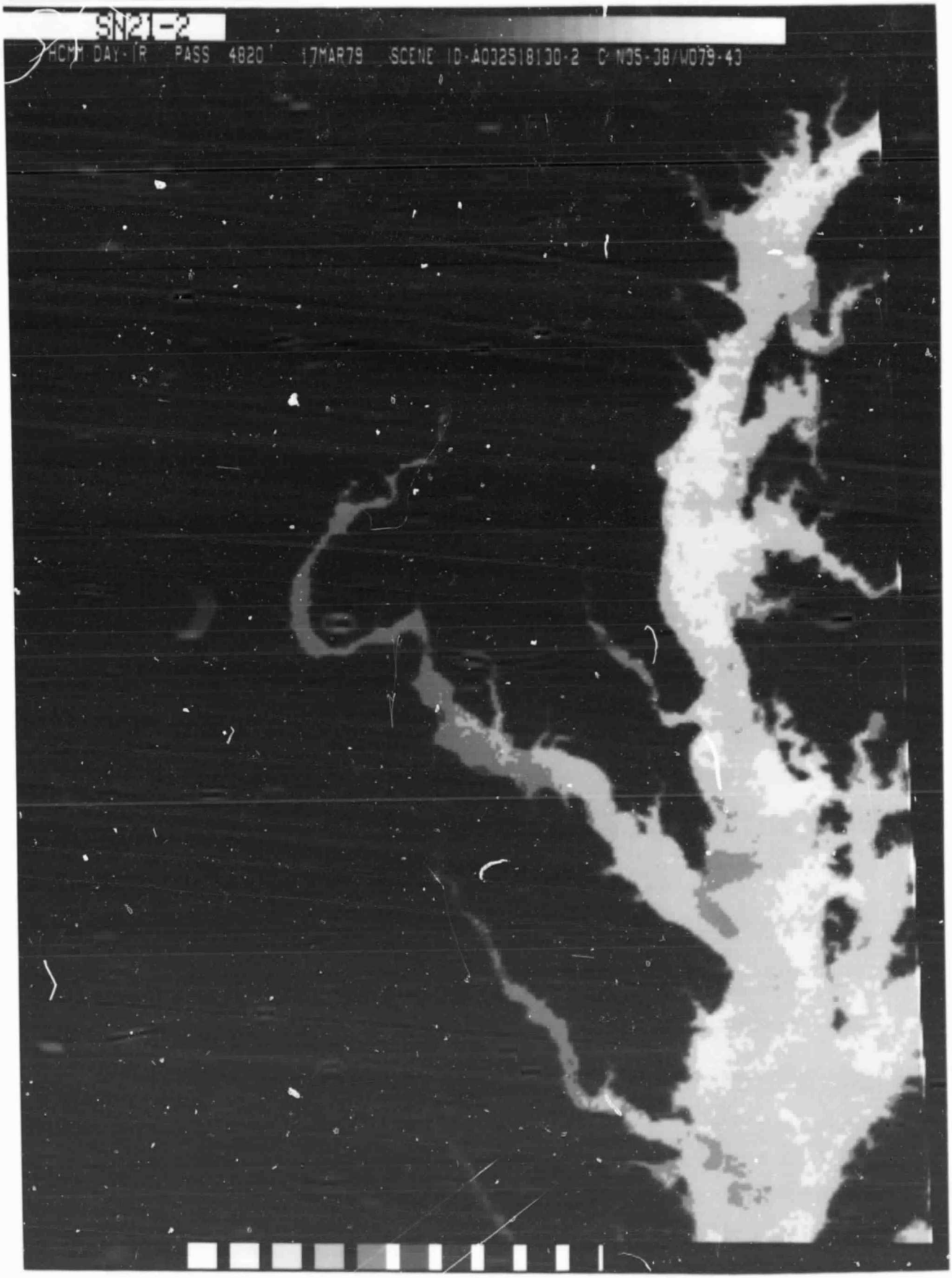

Figure 6. HCMM daytime thermal image of 17 March 1979 (1813Z) (1313 local time). A flood tide is in evidence in the lower estuary. Warm upland water lies off the mouths of the Potomac and the Rappahannock Rivers, discharged by the previous ebb tidal outflow.

have been noted--but not recorded--by the writer in the Merrimac River estuary of Massachusetts (Wiesnet and Cotton, 1967). An experiment to identify these water masses and verify their existence is highly recommended. Aircraft could be utilized to monitor the movement and assimilation of these presumably somewhat polluted river-discharged water masses.

It is further speculated that pollutants from the easterly flowing rivers into the Chesapeake Bay would result in concentrations of pollutants along the western shore that were higher than those on the eastern shore. Slugs of water discharged from the Potomac are warmer and less dense and hence will float as identifiable water masses retaining their characteristics for some undertermined time. It is possible to track these slugs of water by aircraft equipped with thermal scanners of appropriate sensitivity. Efforts to study the Chesapeake Bay plume in 1980 did make use of aircraft that were equipped with thermal radiometers and other instruments as well (Janet Campbell, 20 November 1980, informal communication).

Using a NOAA computer program, a series of microfilm printouts was prepared from the 17 March 1979 HCMM CCT's (Fig. 7). Assembling these arrays of thermal data, on which isopleths had been automatically drawn by an IBM-360 program, a thermal map of the data over the lower Potomac was prepared as a mosaic. It outlines the river well, except at the very mouth.

Fig. 8 is an illustration of the quantitative capability of the HCMM printout. These temperatures are based on preflight calibration data, not the absolute temperatures. However, the temperature differences are significant. The river flow is at ebb as described previously. Ordinarily, the river constriction produces great turbulence as the water is squeezed through the narrows. Yet the printout shows the temperatures to be higher than those above and below. The location of a power plant is shown by the black square. It is

"Page missing from available version"

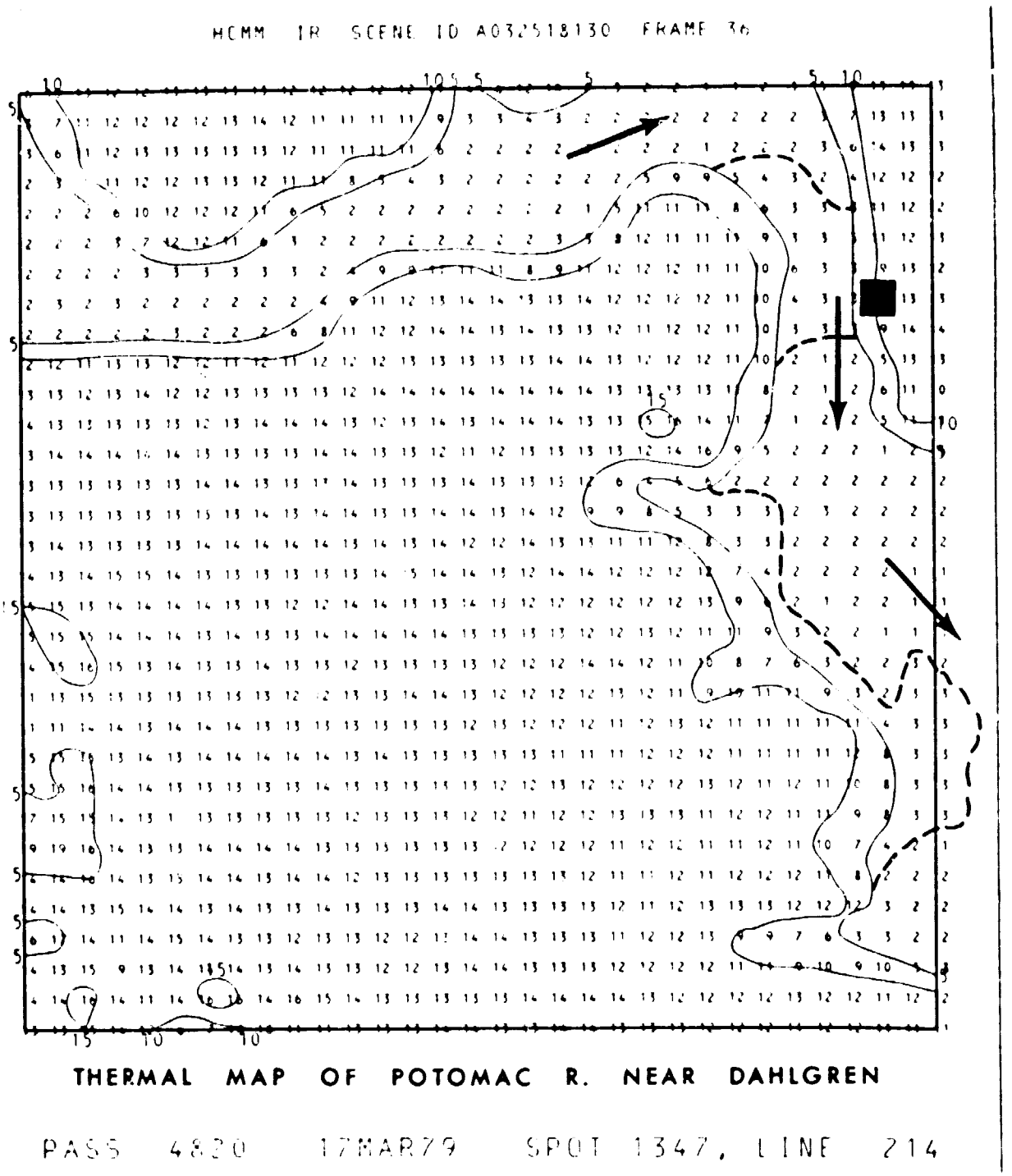

Figure 8. Thermal surface digital map of the narrows at Big Bend in the Potomac River showing the location of the power plant and the direction of flow.

just south of the U.S. Route 301 Potomac River Bridge.

The higher temperatures recorded by the HCMM HCMR may be due to:

1. pixel contamination by land portions.
2. pixel contamination by the U.S. Route 301 Bridge.
3. warm water produced either naturally, or by the outflow from the steam-generating plant.

We believe the most likely explanation is that while all three causes play a role, that the wide spread nature of the warming indicates the third cause is the most important. If this is true, the HCMM satellite has demonstrated its ability to detect even the small rise in temperature caused by the power plant effluent.

COOPER RIVER

The port of Charleston, S.C., is a commercial and naval shipping center located at the confluence of the Cooper River, the Wando River, and the Ashley River (Fig. 9). In 1967, an extensive effort was made to study the tidal current circulation patterns in this complex estuary by means of photogrammetric methods (U.S. Dept. of Commerce, 1967).

Despite the small size of this estuary, it was decided to attempt a study under what we regarded as "worst-case" conditions. That is, only a few HCMM pixels would be discernible. The thesis was that given a sufficient Δt between sea water and upland (fresh) water, it should be possible to detect the tidal stage and perhaps infer generalized current patterns from the thermal pattern in the estuary. We had requested--but failed to receive--aircraft overflights that would have provided synoptic thermal maps at "great" or at least reasonable detail. In fact, one scientist on the selection panel was quite skeptical about this test site. The scientist stated "The panel knew that your real

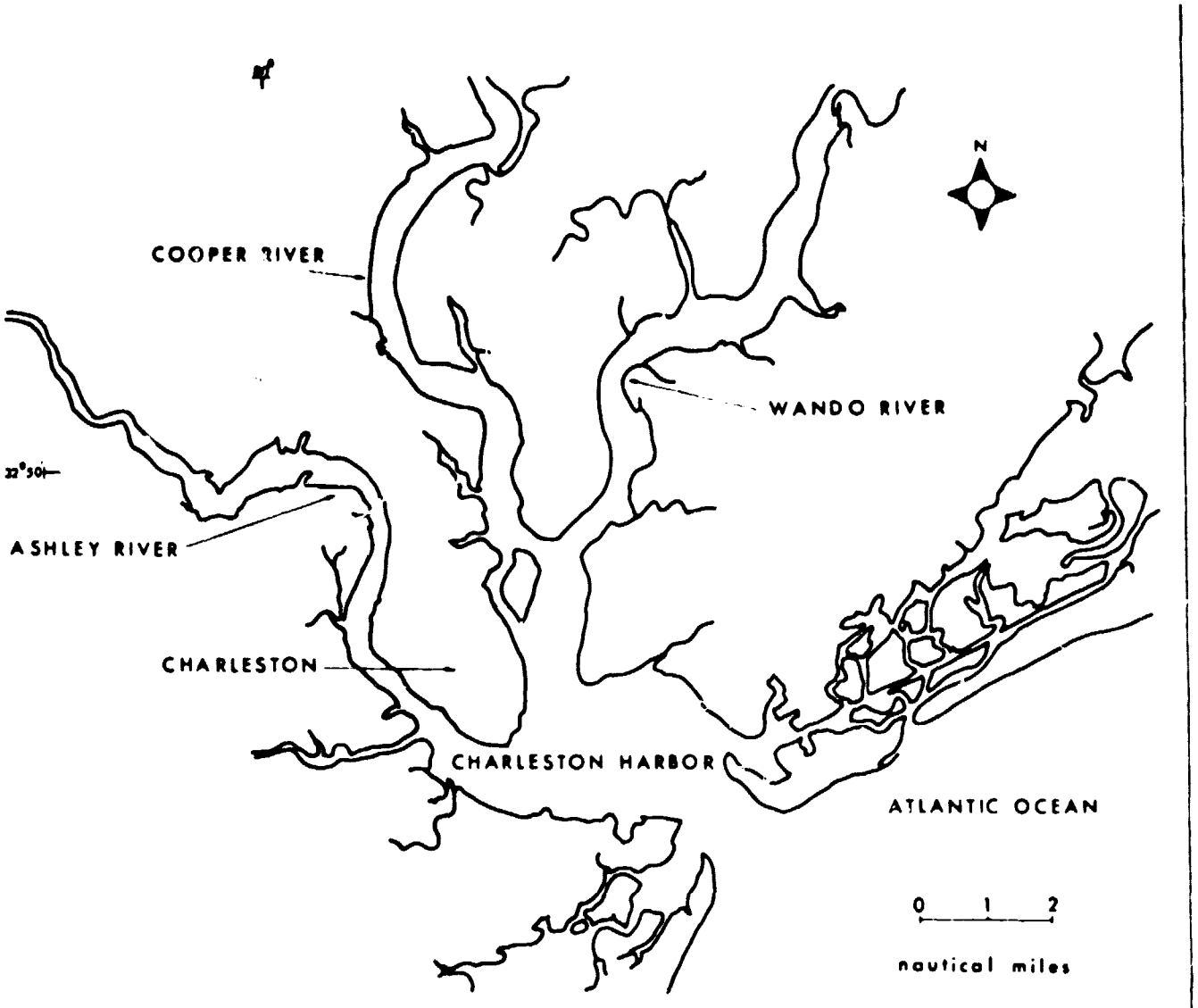

Figure 9. Index map of the Cooper River test site showing localities mentioned in the report.

interest was in securing the aircraft imagery, because you'll get only a half dozen pixels from the satellite, and that won't show you a thing." The panel scientist's comment was partly correct, but we did hold out some hope for the satellite data.

Fig. 10 is a printout of raw values that delineates the estuary on 10 Jan. 1979 (nighttime Scene ID A025906550). The scene has been isolined at 10, 20, and 30 counts--raw data values. Note that the three rivers, the Cooper, the Ashley, and the Wando--are detectable. Note also the warm sea water and the much cooler upland water. Coldest of all are the land surface areas. We interpreted the pattern as indicating a mid-flood condition. Tide tables were used to determine that the scene was recorded 3 hours after low tide at the Charleston Harbor entrance, thus verifying our interpretation. It is felt that this chart has furnished proof of concept that the HCMM HCMR can monitor tidal changes in small estuaries under appropriate thermal and atmospheric conditions.

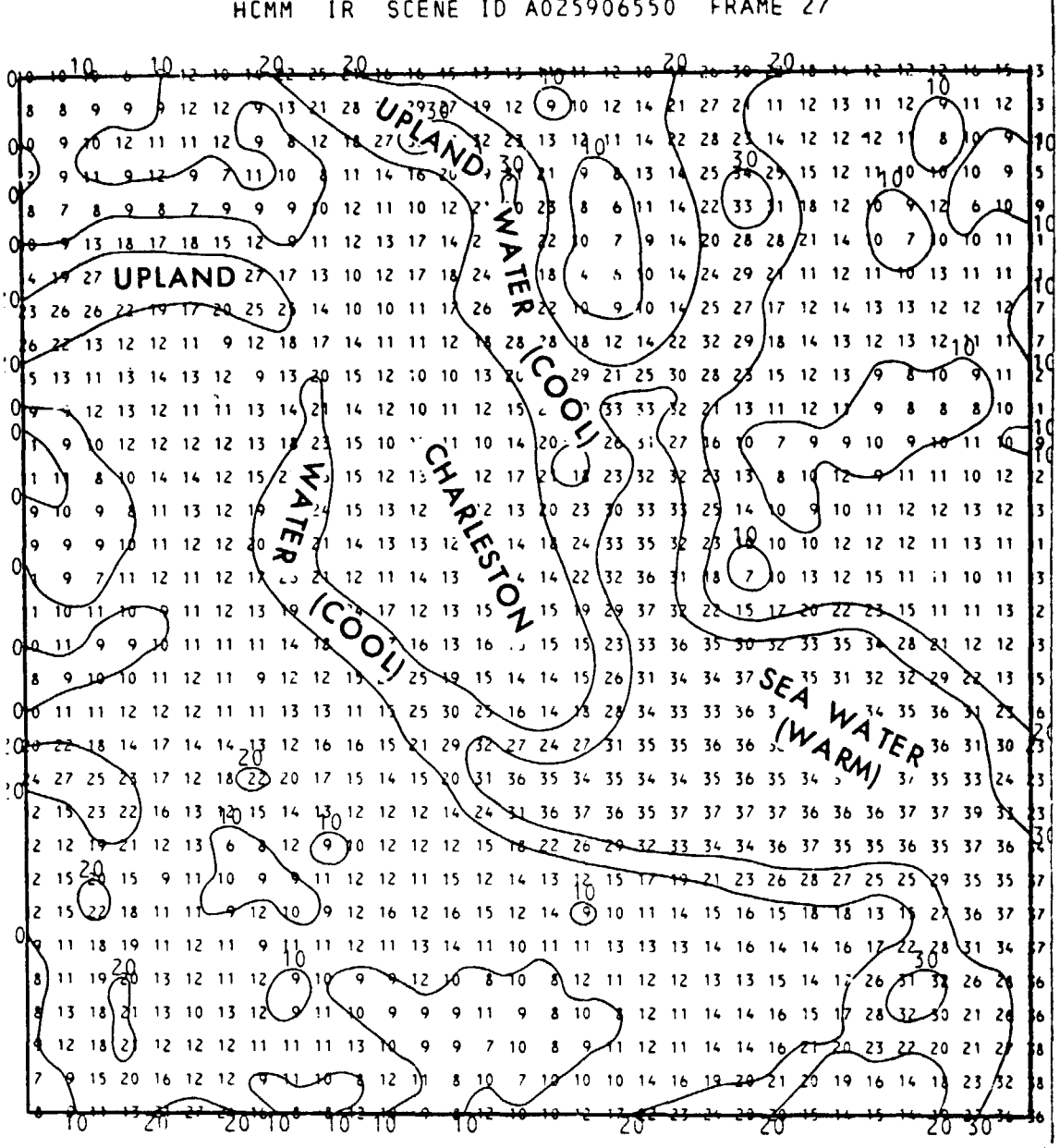

Figure 10. Thermal surface printout of uncorrected digital count values showing the ability to distinguish water temperatures and to determine tidal stage (flood).

REFERENCES

Hartwell, A.D., 1970, Hydrology and Holocene Sedimentation of the Merrimack River Estuary, Massachusetts, Univ. of Mass., Dept. of Geology Contrib. No. 5 CRG, 166 pp. (ONR Geog. Br. Contract Rept. NONRN 00014-67-A-0230-0001).

Klemas, V., Otley, M., and Wethe, C., 1974, Monitoring Coastal Water Properties and Current Circulation with ERTS-1 Third Earth Res. Tech. Satellite-1 Symp., Greenbelt, Md., NASA SP-351, pp. 1387-1411.

Mairs, R.L. and Clark, D.K., 1973, "Remote Sensing of Estuarine Circulation Dynamics," Photogramm. Eng., V. 34, No. 9, pp. 927-938.

NOAA, 1979, Tidal Current Tables, 1979 Atlantic Coast of North America, U.S. Dept. of Commerce, NOAA, NOS, 218 pp.

Price, J., 1981, "The Contribution of Thermal Data in Landsat Multispectral Classification," Photogramm. Eng., V. 47, No. 2, pp. 229-236.

Pritchard, D., 1967, "Observations of Circulation in Coastal Plain Estuaries," in Lauff, G.H., Estuaries, Pub. No. 83, AAAS, Washington, D.C.

U.S. Dept. of Commerce, 1967, Tidal Current Charts, Charleston Harbor, S.C., 12 Charts, ESSA, C&GS, Rockville, Md.

Wiesnet, D.R., 1972, "Quasioperational Current Mapping by Thermal Infrared in South Korean Coastal Regions," Coastal Mapping Symposium, Amer. Soc. Photogramm., Washington, D.C., 18 pp.

Wiesnet, D.R. and Cotton, J.E., 1967, "The Use of Infrared Imagery in Circulation Studies of the Merrimack River Estuary, Mass.," Tech. Letter NASA-78, 11 pp., U.S. Geological Survey Admin. Report.

PART B: SOIL MOISTURE

INTRODUCTION

The crude approximations for soil moisture used in hydrologic design (USDA, Soil Conservation Service, 1957) and streamflow estimates (Burnash, et al., 1973) demonstrate the need for improved soil-moisture estimates. Most soil moisture values are actually based on weighted or accumulated precipitation measurements from rain gages. Soil-moisture measurements are rarely taken in situ and when taken, represent point values that are not likely a representative indication of true basin soil moisture. There is a real need for areally averaged soil moisture values that accurately reflect the condition of the watershed and its response to rainfall.

CONCEPT OF THERMAL INERTIA

One of the techniques that provides soil moisture information is thermal inertia. Thermal inertia is a measure of the resistence of matter to a change in its temperature. As explained by Gillespie and Kahle (1977) thermal inertia is a volume property and can thus sense below the ground surface, permitting discrimination among different materials whose surfaces are similar. With regard to soil moisture, for a given soil, changes in its moisture profile will result in thermal-inertia changes. The high specific heat of water (much higher than the soil) results in increased thermal inertia as soil-moisture content increases.

In terms of changes in surface soil temperatures, high thermal inertia (wet soils) produces a small diurnal variation or amplitude of temperature; low thermal inertia (dry soils) produces a large diurnal variation. Thermal inertia changes are affected by the amount of moisture in the soil, distribution of moisture within the profile, soil type, sun angle, and vegetative cover.

OBJECTIVE OF THE STUDY

The objective of the study was to evaluate the thermal-inertia technique

for soil moisture. The HCMM satellite was launched in orbit to provide, at regular intervals, night and day coverage of a given location near the time minimum and maximum surface temperatures are generally encountered (approximately 0200 and 1300 LST), times critical for the evaluation of thermal inertia.

SELECTION OF A TEST SITE-LUVERNE MINNESOTA

The Luverne, Minnesota, test site (Fig.'s 11 and 12) has been used for NOAA gamma ray airborne experiments with an established network of soil sampling sites since the spring of 1969 (Peck, et al., 1971). At present local Soil Conservation Service (SCS) USDA soil scientists are available to collect data upon reimbursement by the NOAA under a NWS contract. The area comprises flat to rolling farmland with few trees. During spring (April to early June) large tracts (65 to 260 hectares, 160 to 640 acres) are planted principally with corn and soybeans. These fields remain bare until emergence of the crop which may take from one to three weeks depending upon weather conditions and type of crop. With a pixel resolution of 0.6 x 0.6 km in the infrared, the HCMM Heat Capacity Mapping Radiometer (HCMR) could image areas as small as 36 hectares (90 acres). Thus these large bare tracts could fill as many as seven pixels and therefore be monitored by the HCMR on board HCMM.

The site would provide ground truth for satellite overflights in which thermal data were collected and thermal inertia maps were prepared. Repeated observations during spring (bare fields), summer (vegetative fields), and fall (fallow, harvested fields) would provide material for evaluation and comparison with thermal data. It was hoped that HCMM data plus ground observations would also provide information on the more complex signature of activly growing crops plus soil moisture.

RSG ½ GAGE

To provide a continuous source of information regarding changes in soil moisture at the Luverne, Minnesota, test site, an RSG½ snow and soil moisture gage

Figure 11. Location of Luverne, Minnesota.

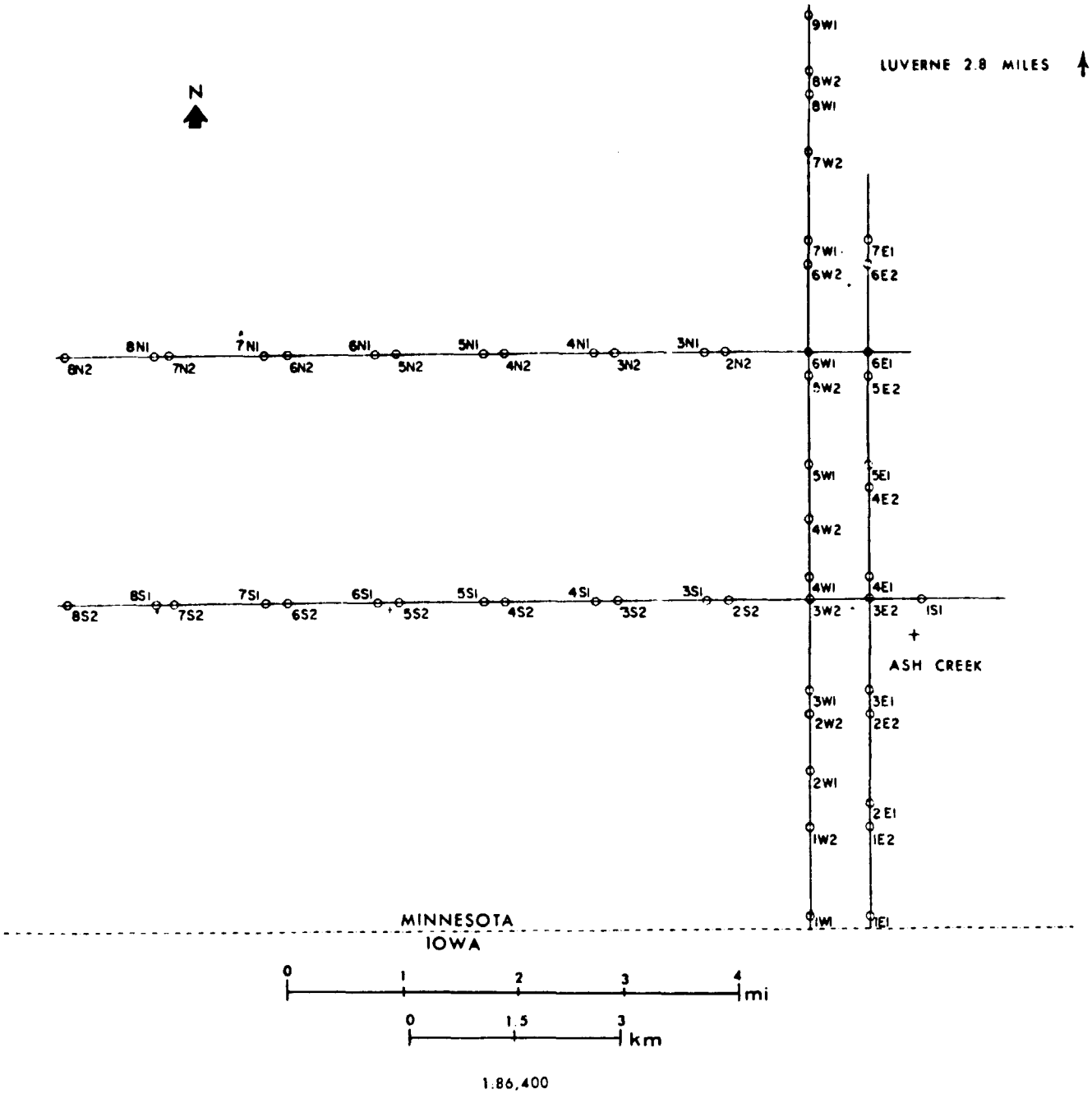

Figure 12. Location of flight lines at Luverne, Minnesota test site.

was installed in December 1978. The gage site is located on flight line W (Fig. 12), approximately 1 km (0.6 miles) north of the Iowa-Minnesota border at the crest of a small hill, 15 meters west of U.S. Route 75. In December, 1979 a LaBarge data collection platform (DCP) was linked electronically to the RSG½ gage to provide soil moisture from 0 to 10cm (0 to 4 in), snow water equivalent, air temperature, and battery voltage daily at 6-hour intervals. Such information is transmitted via the GOES (Geostationary Operational Environmental Satellite) to computers in the World Weather Building in Camp Springs, MD. Unfortunately the desired data have been difficult to obtain, as a result of equipment failures and calibration delays. This failure precluded an analysis of whether a single data point could be related to average soil moisture conditions along a flight line or over a region. Such a relation would be useful in relating ground information, based on a single point, to the 0.6 km HCMR data and a possible thermal inertia relationship.

SELECTION OF HCMM COVERAGE

Data from the months of February, March, August, October and November gave coverage during dormancy, peak growing season, and post-harvest--a large variety of surface conditions for thermal-inertia evaluation. Though the test site was viewed by the HCMM satellite on five days in the 16-day cycle, cloud cover as well as data acquisition problems limited the data actually available. Table 1 provides pertinent information regarding coverage for the Luverne soil moisture study. During the first cycle of 13 months only one third of the day scenes received were clear; half of the night images were clear. The fall and winter months had a much higher incidence of cloud cover than August. Overall, of the total possible scenes (67 day and 67 night) only 15 days (22%) and 17 nights (25%) were sufficiently devoid of clouds to be useful for analysis--rather discouraging. Only six pairs of image sequences (night/day) received were clear and have potential use for thermal inertia. The only sequence,

Table 1. HCMM Coverage of Luverne, Minnesota Test Site, 4/27/78 - 5/31/79

Month	Total Possible Scenes		No. Scenes Processed		No. Scenes Received		No. Received Clear	
	Day	Night	Day	Night	Day	Night	Day	Night
August	14	14	12	11	8	11	4	7
Oct-Nov	27	27	25	23	21	20	6	9
Feb-Mar	26	26	19	4	14	2	5	1
Total	67	67	56	38	43	33	15	17

when adequate ground and aircraft data were collected, 13 June 1979, was negated when the nighttime pass could not be processed by NASA.

LITERATURE REVIEW

Satellites and aircraft offer remote platforms that have the greatest potential for basin-wide soil moisture estimates. Sensors scanning in such portions of the electromagnetic spectrum as the near-IR (Merritt and Hall, 1973), thermal (Idso, et al., 1975, Jackson, et al., 1976), gamma ray (Feimster, et al., 1975) and microwave (Schmugge, 1976b; Schmugge, et al., 1976a; Schmugge, et al., 1976b; Wang, et al., 1980) have been used in an attempt to obtain basin-wide soil moisture. An extensive study of active microwave work with soil moisture has been done by Batlivala and Ulaby (1977), while work by Schmugge, et al. (1976a) covers the passive microwave area. Unfortunately the resolution of satellite-borne passive microwave data is currently limited to approximately 25 km. A paper by Schmugge, et al. (1980) summarizes various methods for soil moisture determination, including in situ as well as remote sensing techniques currently in use. Wiesnet et al. (1978) studied the use of Landsat MSS data to estimate soil moisture in Phoenix, Arizona, and Luverne, Minnesota.

A short survey paper by Blanchard, et al. (1974) discusses the possibility of using remote thermal measurements of soil surfaces to assess seasonal soil moisture changes to depths of 10cm. The authors caution that remote radiometric temperature measurements of soil do not equal actual soil temperatures because soils have emissivities less than one (0.7 to 0.9 depending on texture, grain size, and mineralogy). Soil emissivity increases as soil moisture increases (Fuchs and Tanner, 1968). However, for the same soil type and given conditions, radiometrically, measured temperature changes are the same as actual changes.

Extensive studies conducted at the U.S. Water Conservation Laboratory in Phoenix, Arizona show the utility of surface temperature measurements for the remote sensing of surface (up to 4cm depth) soil moisture. Idso et al. (1975) found good correlation between the amplitude of the diurnal soil temperature wave (i.e. Tsoilmax-Tsoilmin) and the volumetric soil water content for Avondale loam soil (see Figure 13). Unfortunately the same relationship could not be varified for other soil types such as Navajo clay, gran sandy loam, and cashion silty clay. However, by using the moisture characteristic curves of each soil to transform water content into pressure potential (see Figure 14), it was found that soil water pressure potential could be determined without prior knowledge of soil type (See Figure 15) thereby significantly enhancing the value of thermal inertia as a potential global soil water survey tool.

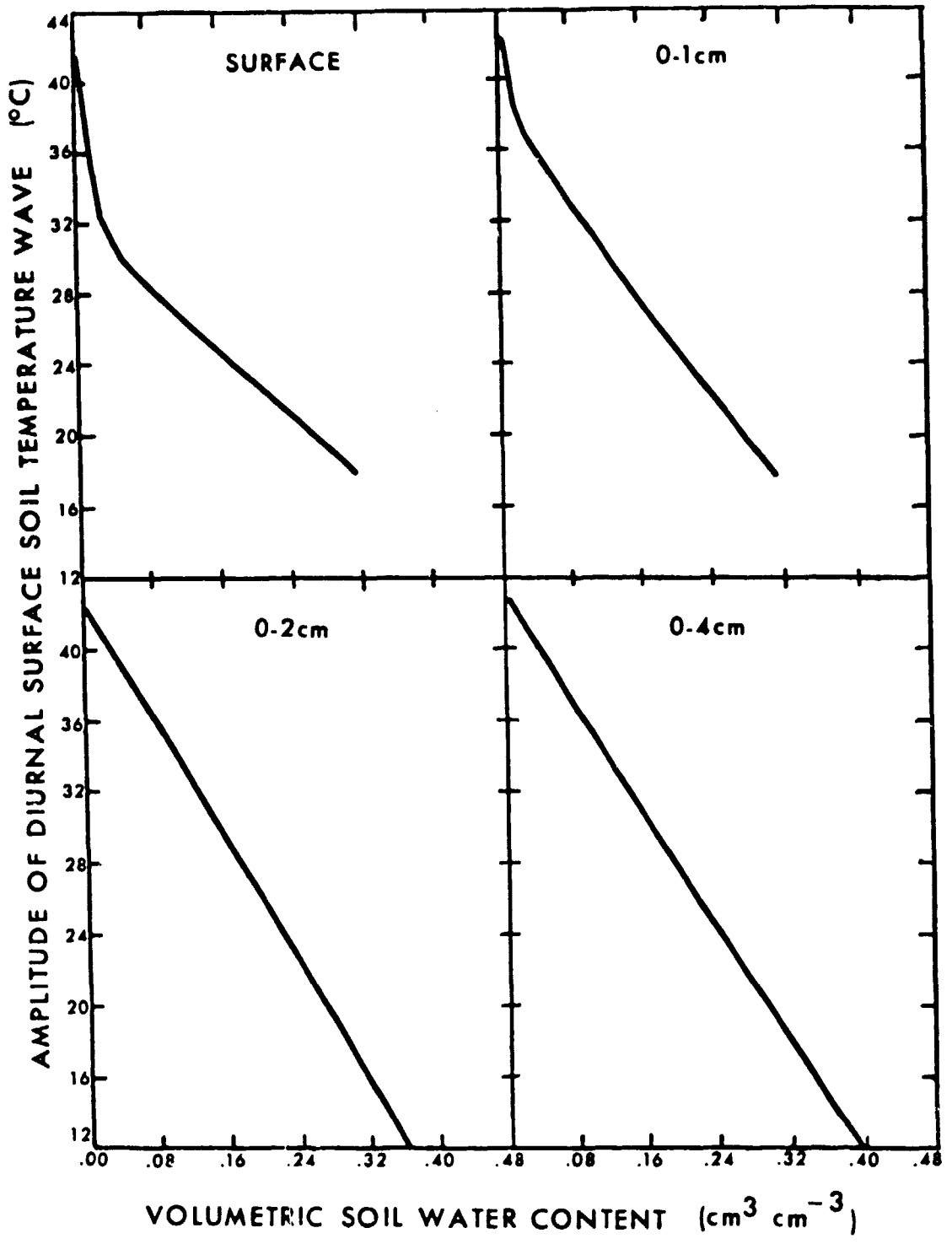

Figure 13. Amplitude of diurnal surface soil temperature wave vs. volumetric soil water content (After Idso, et al., 1975).

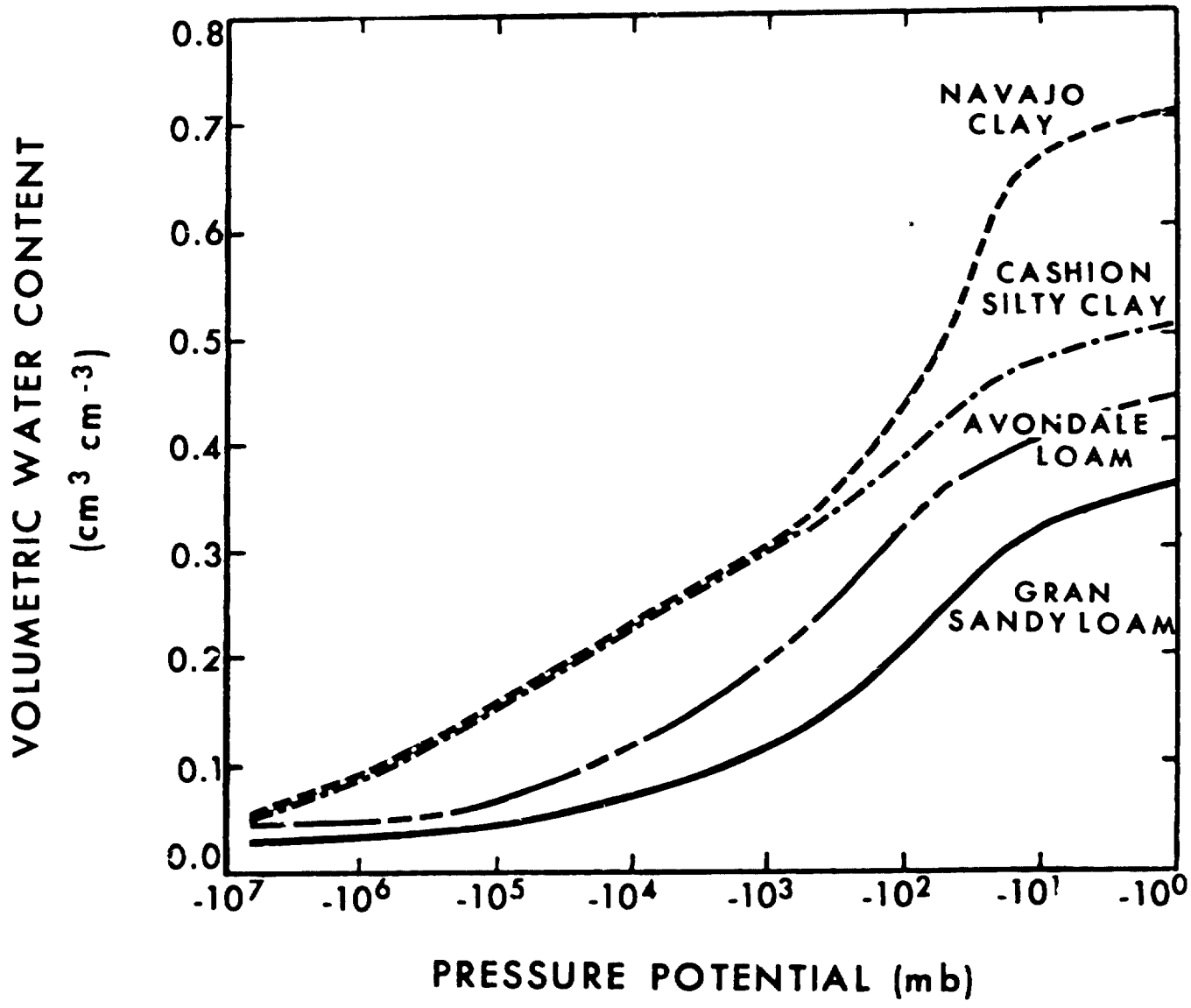

Figure 14. Volumetric soil water content vs. soil water pressure potential for four different soils (After Idso, et al., 1975).

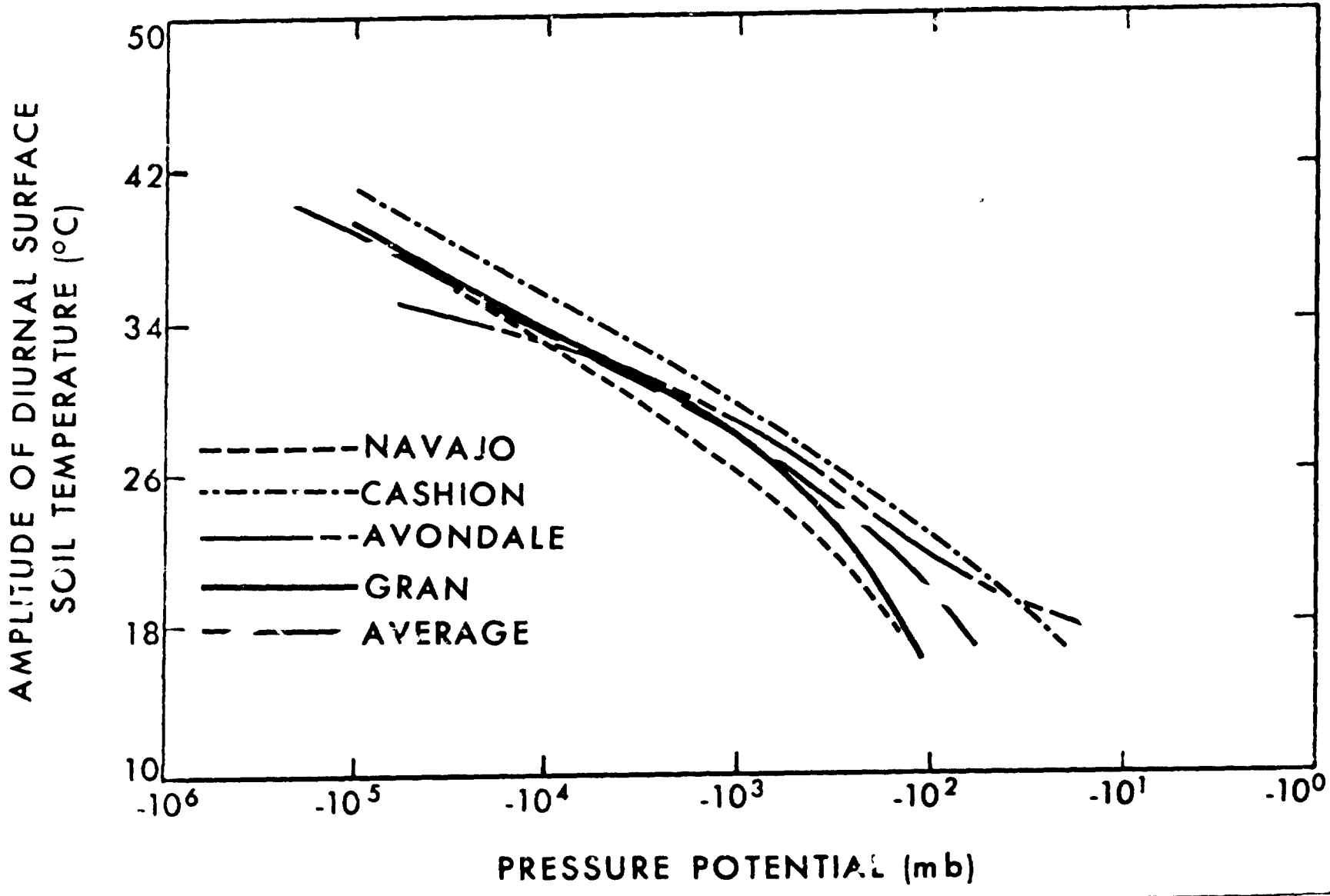

Figure 15. Amplitude of diurnal surface soil temperature wave vs. mean daylight soil water pressure potential of the 0-2-cm depth for four different soils (After Idso, et al., 1975).

FIELD SURVEYS

Primary field surveys for data collection were held on 20 October 1977, 20 May 1978, and 13 June 1979. Secondary efforts were scheduled for 19 December 1978, and 6 December 1979 to coincide with the RSG½ soil moisture gage installation and the data collection platform installation, respectively.

20 October 1977

The purpose of the 20 October 1977 Luverne experiment was to collect sufficient ground information to evaluate the aircraft (U-2) HCMR data, which was to be flown concurrently. It was a typical prelaunch experiment designed to test the instruments and techniques specified and locate any problems that might develop.

The field party consisted of four persons, two from NOAA/NESS (Wiesnet and McGinnis) and two from the SCS at Marshall, Minn. (Hokanson and Nelson).

A recording meteorological station was set up on the test site. Wind direction, wind speed, air temperature, and relative humidity were continuously recorded at this site. Additional daily data for the preceding month were obtained from the local NWS cooperative observer.

On the survey date (20 Oct) a total of 18 soil moisture samples were collected; soil temperatures at the surface and at depth, via a probe (0-5cm), were taken at each sampling site. Sample sites included:

1. bare soil
2. soybean field
3. cornfield (standing corn)
4. cornfield (stubble)
5. disked field
6. plowed field
7. soybean stubble

On 21 October Wiesnet and McGinnis extended the ground-based observations by taking 8 more samples and temperatures. This made a total of 26 soil moisture samples. The location of these samples is shown in Figure 16. Note that the collection time of each soil sample is given in CDT. Collection sites without dates were sampled on 20 October. Sites marked by an 'X' only were sampled during the morning of 20 October between 0900 and 1200.

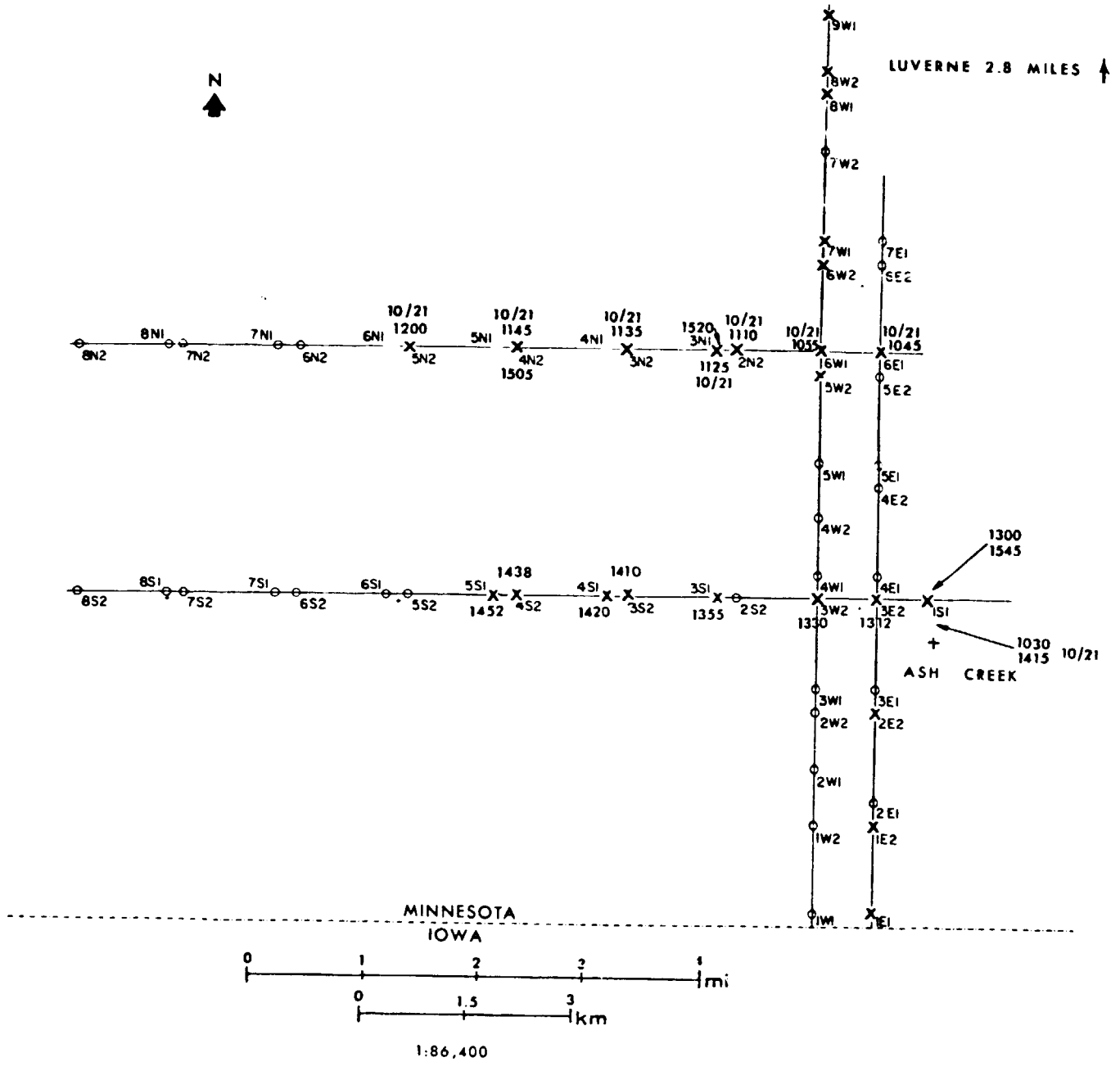

Figure 16. Location of data sampling points at Luverne test site, 10/20/77.

Skin temperature ranged from 23.0°C to 31.0°C on 20 October; from 16.5°C to 25.6°C on 21 October. Soil temperature at depth (5 cm) ranged from 9.8°C to 15.9°C on 20 October, and from 8.4°C to 13.9°C the following day.

Soil moisture values were obtained from the Twin City Testing Laboratory, Sioux Falls, S.D. They ranged from 19.6% to 49.2% on 20 October, and from 21.6% to 28.0% on 21 October.

Air temperature ranged from 19°C to 21°C during the period of data collection on 20 October, and from 9°C to 10°C on 21 October.

Two problems were noted: (1) a drive or clock mechanism on the weather station drum was not accurate and (2) some of the probe measurements were apparently done without waiting for the probe to reach equilibrium with the deeper soil temperature. Both problems are correctable.

20 May, 1978

The purpose of the 20 May 1978 Luverne experiment was to collect soil moisture and soil temperature data coincidental with the early morning and afternoon HCMM satellite overpass. The field party was to consist of four persons, two from the NOAA/NESS and two from the SCS at Marshall, Minnesota. Due to morning cloudiness and the NWS forecast that the cloudiness would persist into the early afternoon, the two SCS personnel were notified that they would not be required to assist in collecting ground data. The clouds, however, dissipated in the late morning and the two NESS personnel proceeded to the test site to collect ground data.

On the survey date (20th May) a total of eight soil moisture samples were collected eight pairs of soil temperatures at the surface and at a depth of 11.5 cm were taken at each sampling site. The location of the samples is shown in Figure 17. Times given are in CDT. Table 2 lists the ground data obtained at each of the eight sites.

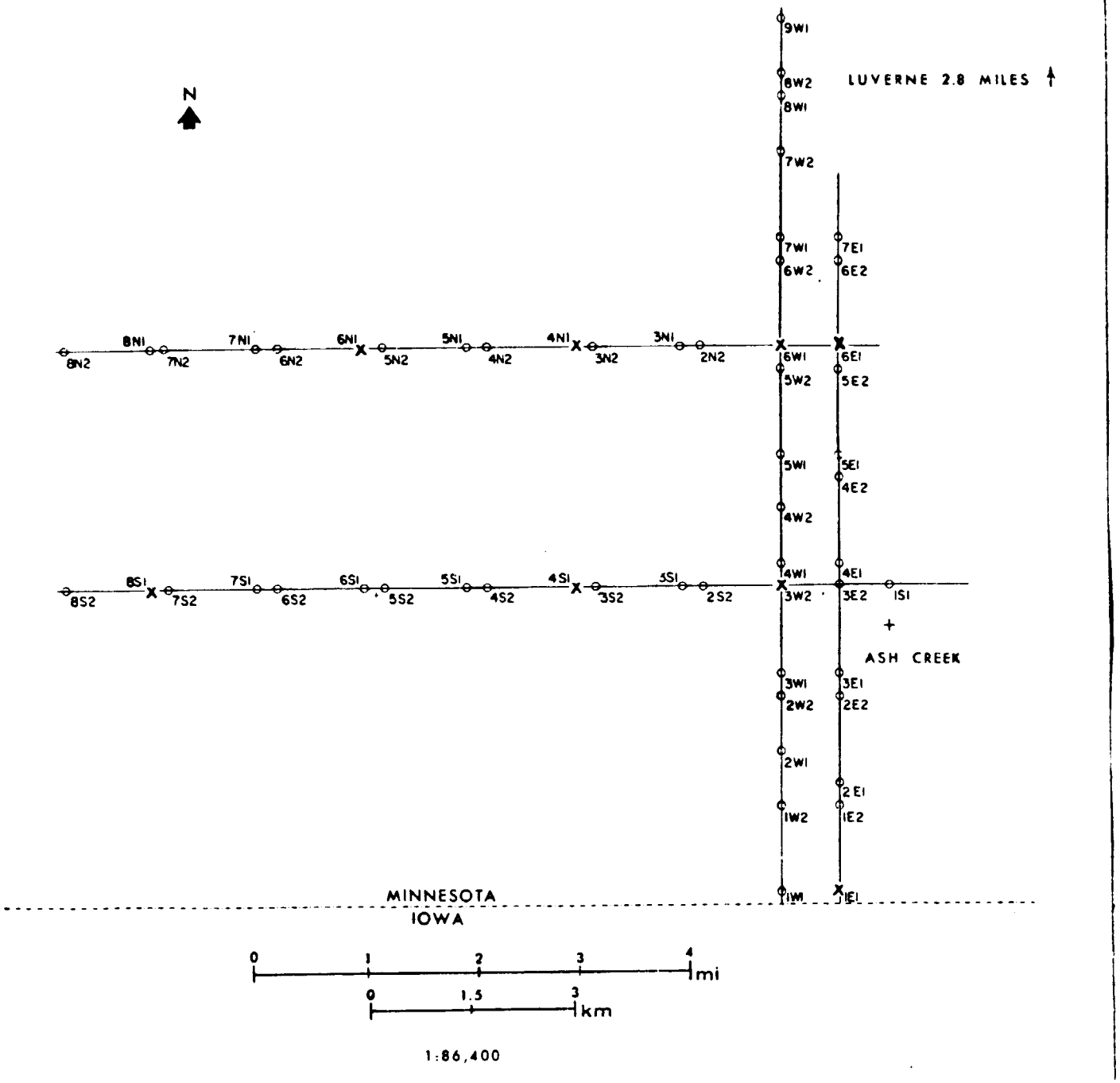

Figure 17. Location of data sampling points at Luverne test site, 5/20/78.

Table 2. Ground data summary for 5/20/78 field survey.

Field ID #	% Soil Moisture	Soil Temp. (°C) Surface	Soil Temp. (°C) 11.5 cm	Air Temp (°C)	Field Description
1E1	25.4	34.8	16.2	21.0	Bare Field
3D1	31.7	30.9	14.6	20.7	Bare Field
3E1	24.2	26.7	15.2	23.0	Bare Field
3W2	23.3	33.2	14.9	19.0	Bare Field
Wea. Station	19.7	27.5	16.0	18.0	Bare Field
6E1	25.0	33.9	17.9	25.6	Bare Field
6W1	24.3	35.2	16.3	24.8	Bare Field
7D1	20.1	35.2	16.0	23.0	Bare Field

20 December 1978 and 6 December 1979

A problem in over half of the HCMM images of Luverne, clouds prevented collection of useful imagery on 20 December 1978, and during the afternoon of 6 December 1979. Further, the clear predawn HCMM scene of 6 December could not be processed. Fortunately no massive collection of surface and subsurface information had been planned in lieu of the primary mission of gage (20 December 1978) or data collection platform (6 December 1979) installation.

Summary

For the four data collection surveys described above, no useable aircraft data were obtained. HCMM imagery were unavailable due to clouds or could not be processed for the three dates when HCMM was operationally in orbit. Limits in man power and funds prevented further field missions other than that of 13 June 1979.

Detailed Summary of 13 June, 1979 Field Survey

Collection of soil samples, soil temperatures, aircraft, and satellite data.

On Wednesday 13 June 1979, HCMM passed over the Luverne test site on a night/day sequence (0303CT and 1358 CDT respectively). A major data collection effort was carefully planned inconjunction with the HCMM overpasses. The effort involved the cooperation of personnel from NESS and NWS's Office of Hydrology, NASA/JSC and USDA/Soil Conservation Service. Limited ground data, 6 locations only, were collected with the predawn overpass. These data included 10-cm

(4-inch) soil samples, surface temperatues, and 10-cm temperatures. Extensive ground-based data were collected during the day. Over 60 soil samples and 30 sets (surface and 10-cm depth) of soil temperatures were obtained by two, two-man teams between 100 CDT and 1700 CDT. During the collection, four satellites acquired data over the test site: NASA's Heat Capacity Mapping Mission (HCMM) satellite and Landsat-2 and the NOAA-operated TIROS-N and SMS-2 satellites. Data from the four satellites comprised 500-meter visible (055 to 1.1μm) and 600-meter thermal (10.5 to 12.5μm) from HCMM; the four-band Multispectral Scanner Subsystem (MSS) on Landsat at 80-meter resolution in band widths of 0.5 to 0.6μm, 0.6 to 0.7μm, 0.7 to 0.8μm to 1.1μm; the Advanced Very High Resolution Radiometer (AVHRR) on TIROS-N at 1.1km resolution in band widths of 0.55 to 0.90μm, 0.725 to 1.1μm, 3.55 to 3.93μm, and 10.5 to 11.5μm; and the Visible Infrared Spin-Scan Radiometer (VISSR) on SMS-2 at 0.8km resolution in the visible band (0.55 to 0.70μm) and 8.0km resolution in the thermal band (10.5-12.6μm). Aircraft from NASA and NOAA collected data in the visible and thermal-IR and gamma ray portions of the spectrum respectively.

Analysis of data

A portable recording weather station (Meteorology Research Incorporated, Model No. 1087) collected continuous values of ambient temperature, wind direction and speed, and relative humidity. Figure 18 shows the variation of these parameters hour by hour for 13 June 1979. The wind direction was rather constant, prevailing from the west or northwest at all times except at 0300 CDT. The wind speed had a pronounced diurnal variation, being least (less than 10kph) from midnight through 0600 CDT, then increasing to a peak of 26.5 kph at 1300 and 1400 CDT and remaining at or above 20kph until 1700 CDT when the weather station was disassembled. The ambient (air) temperature followed a similar diurnal pattern, reflecting the strong heating of the summer sun under clear skies. Temperatures climbed steadily from a minimum of 8°C (47°F) at 0500 CDT to 27°C

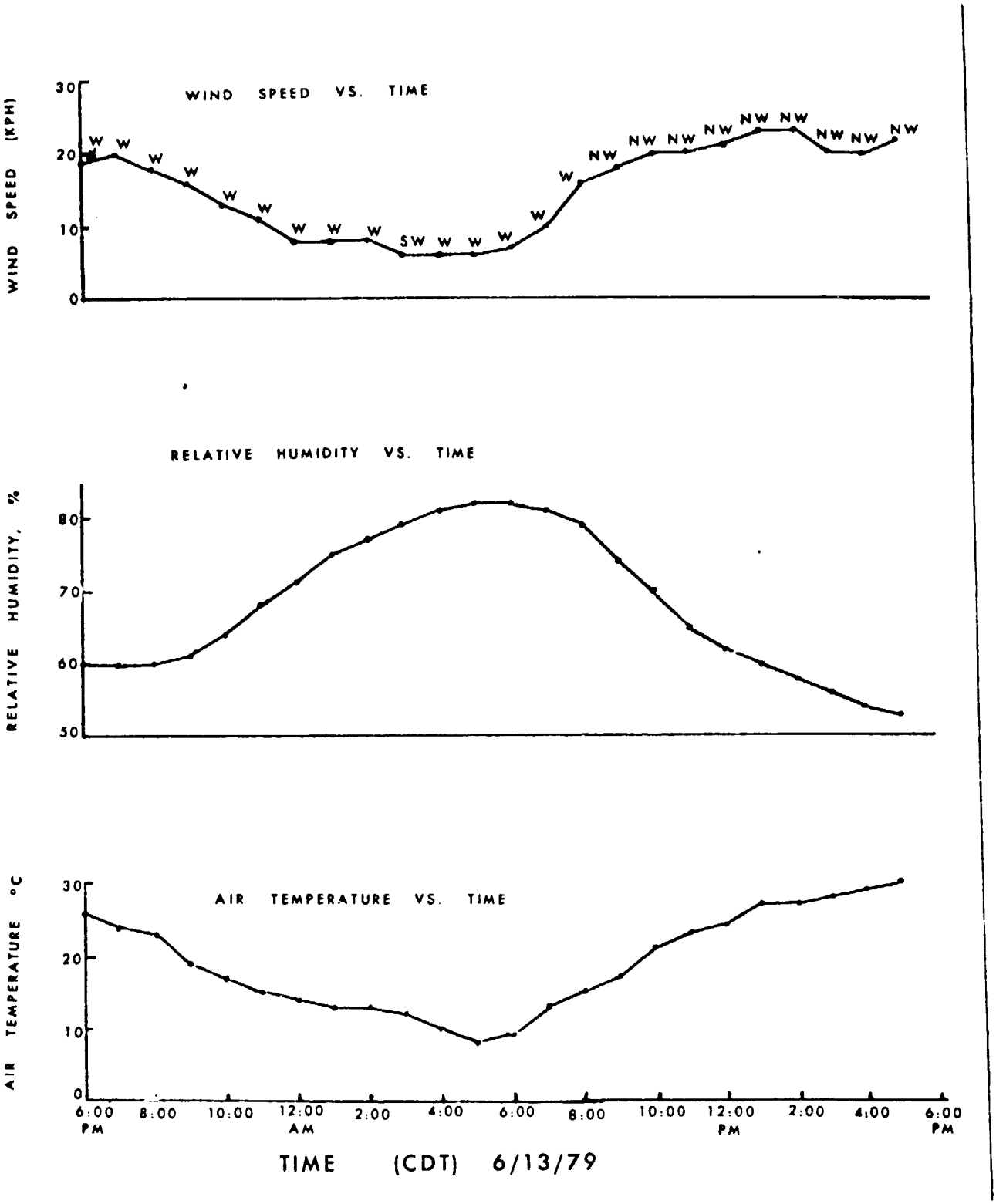

Figure 18. Diurnal variation of wind speed and direction, air temperature, and relative humidity at RSG½ gage site from 1800 CDT 6/12/79 to 1700 CDT, 6/13/79.

(81°F) by 13 CDT. Thereafter the temperature rose slightly to a maximum of 30°C (86°F) at 1700 CDT when the weather station readings were discontinued. As would be expected, the diurnal variation of the relative humidity was opposite that of the temperature, being maximum at 0500 and 0600 CDT, 82 percent, and minimum at 1700 CDT, 53 percent.

Figure 19 shows the variation of land surface temperatures as a function of time. The temperatures were obtained from various points along the flight lines as located in Figure 20. Collection times are given in CDT. A three-point, equal weight moving average (solid line) smooths the variability in the actual data and clearly indicates a rapid warming of the surface (from 34°C to 41°C, 93°F to 106°F) between noon and 1300 CDT. Temperatures remained at this high level (near 40°C, 104°F) during the afternoon, dropping to 38°C (100°F) after 1500 CDT. The variability in the data from the diurnal cycle is likely due to changes in soil moisture, slope, aspect, and/or soil type. The range of soil temperatures at the 10-cm depth (Figure 21) is much less than that experienced at the surface (7°C versus 13°C, 13°F versus 23°F). The 10-cm depth temperature increase occurs more slowly and slightly later than that at the surface, the result of the damping and inertial lag of solar radiation with depth in the soil. Deviations of actual data (dashed line) from the three-point moving average is related to those variables noted previously for surface temperature.

The range of soil moisture content in the top 10-cm (Figure 22) resembles a normal distribution with a slight positive skew. (There are a few values in excess of 32 percent.) When plotted against temperature, soil moisture shows little correlation with surface temperatures, $r^2 = 0.06$, or with 10-cm temepratures, $r^2 = 0.19$ (Figures 23 and 24). An analysis of the ground data showed that soil moisture variations are also independent of elevation.

The gamma ray flights coordinated by Dr. Thomas Carroll, National Weather Service, River Forecast Center, Minneapolis, Minnesota, resulted in soil mois-

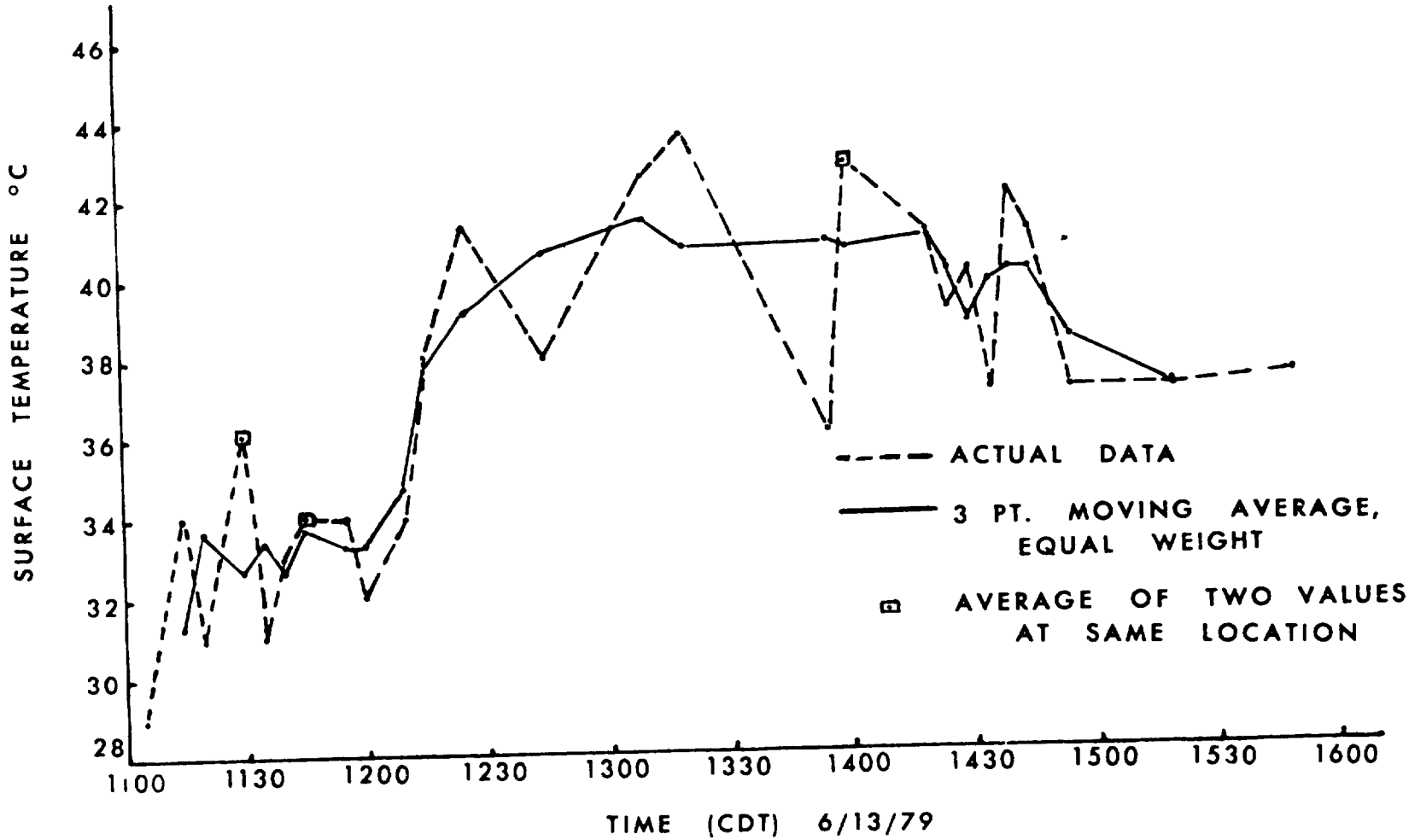

Figure 19. Variation of surface temperatures at Luverne test site, 6/13/79.

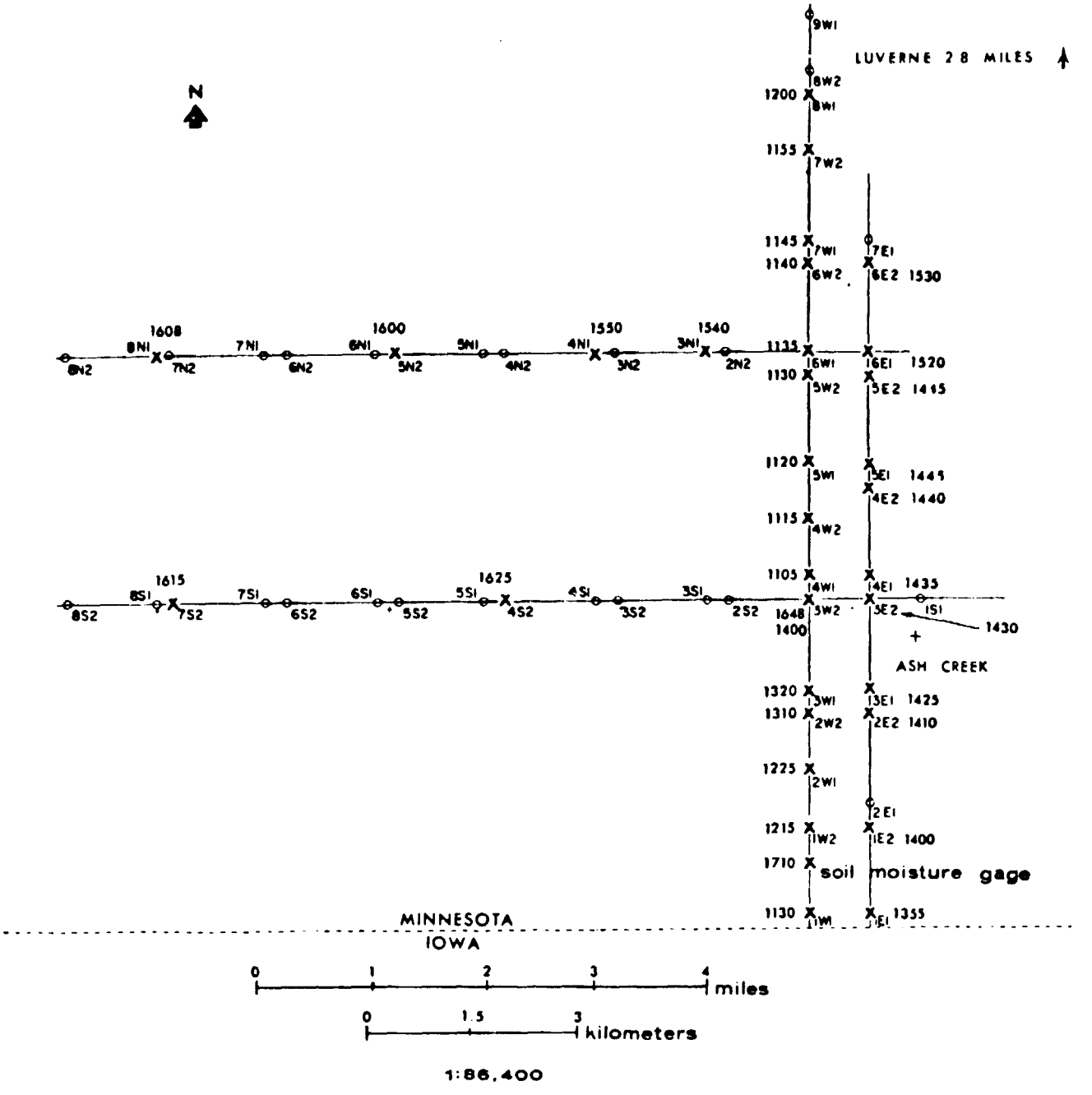

Figure 20. Location of data sampling points at Luverne test site, 6/13/79.

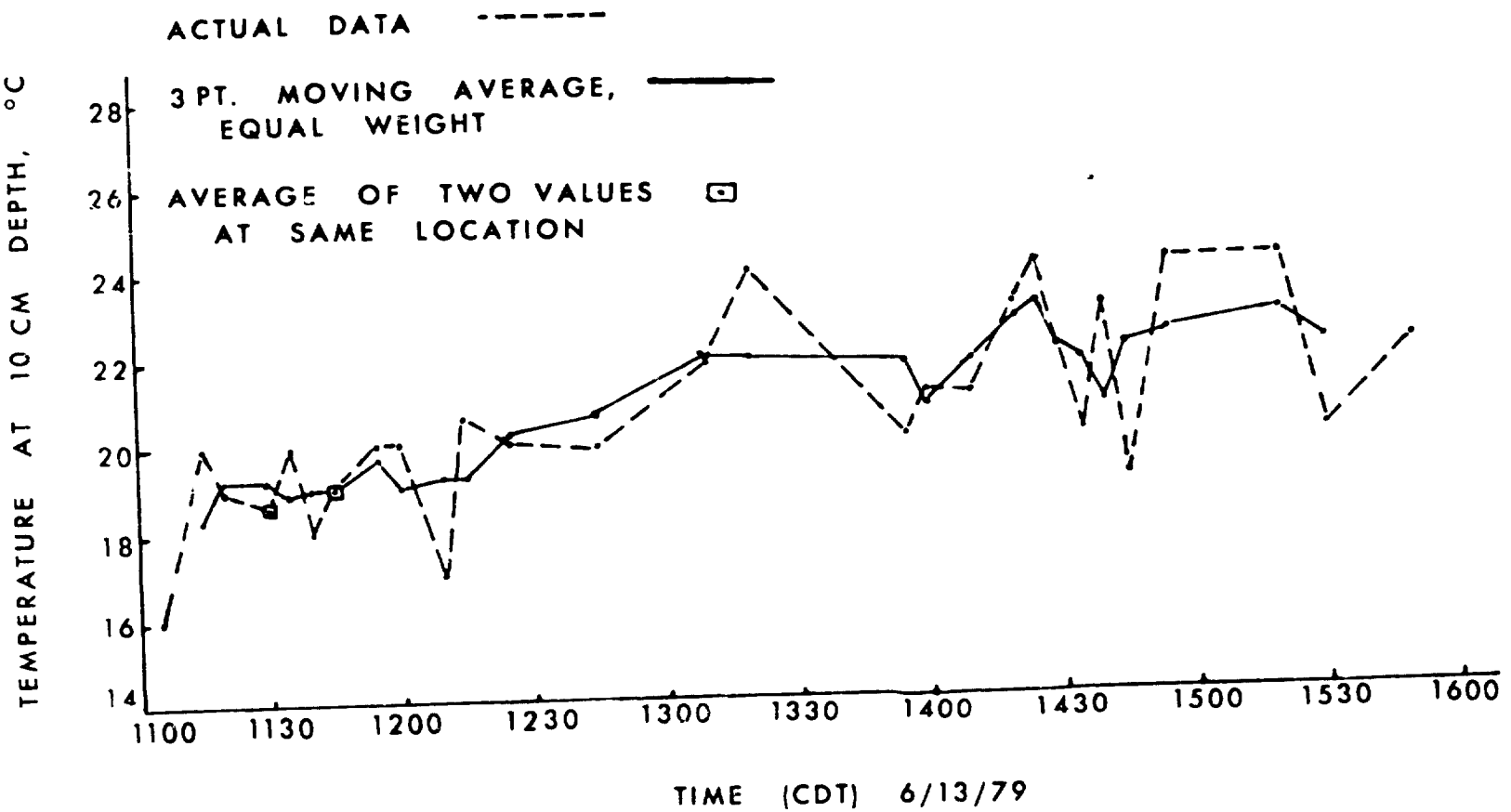

Figure 21. Variation of temperatures at 10-cm depth at Luverne test site, 6/13/79.

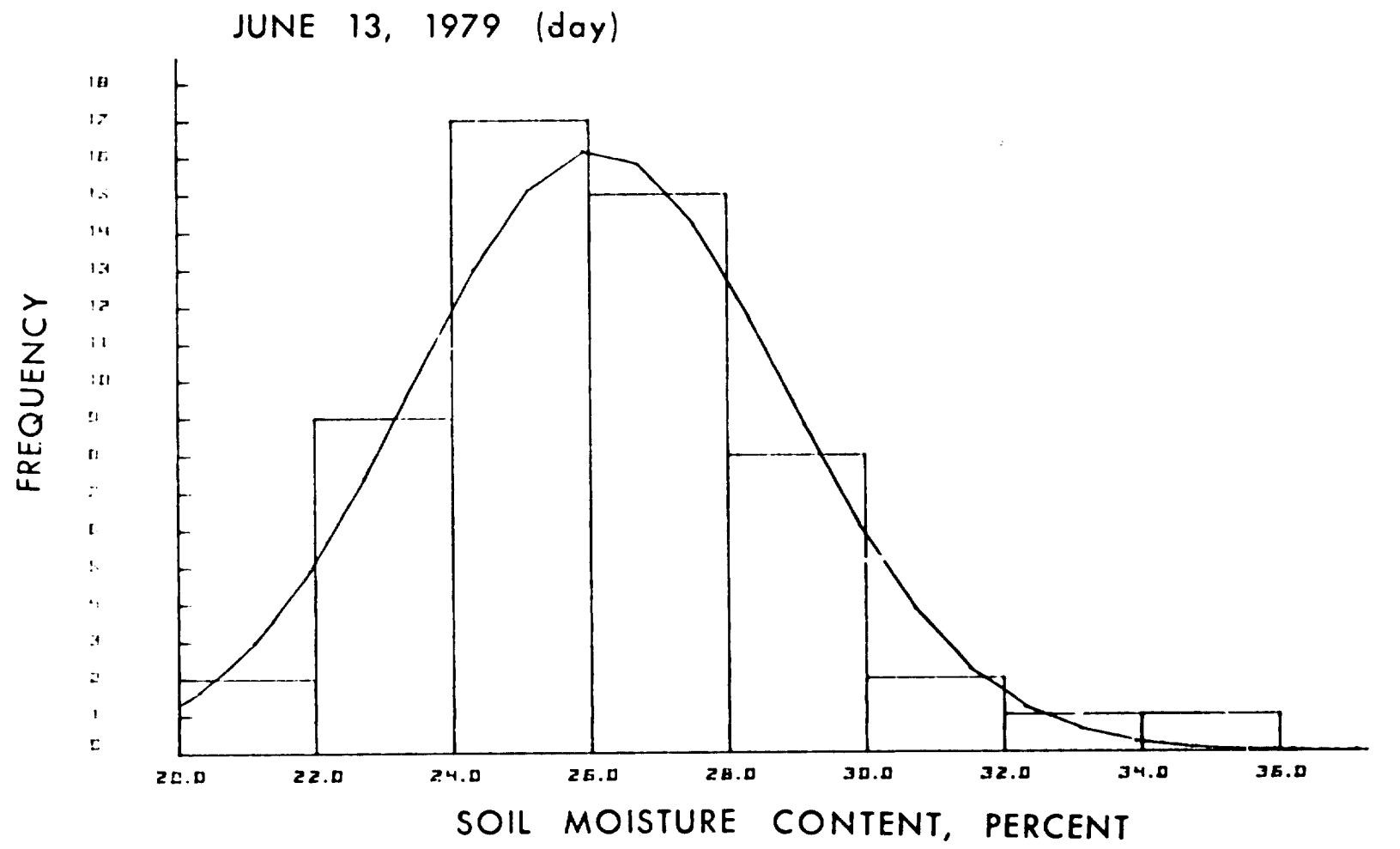

Figure 22. Distribution of soil moisture content, in percent, of soil samples collected at Luverne test site, 6/13/79.

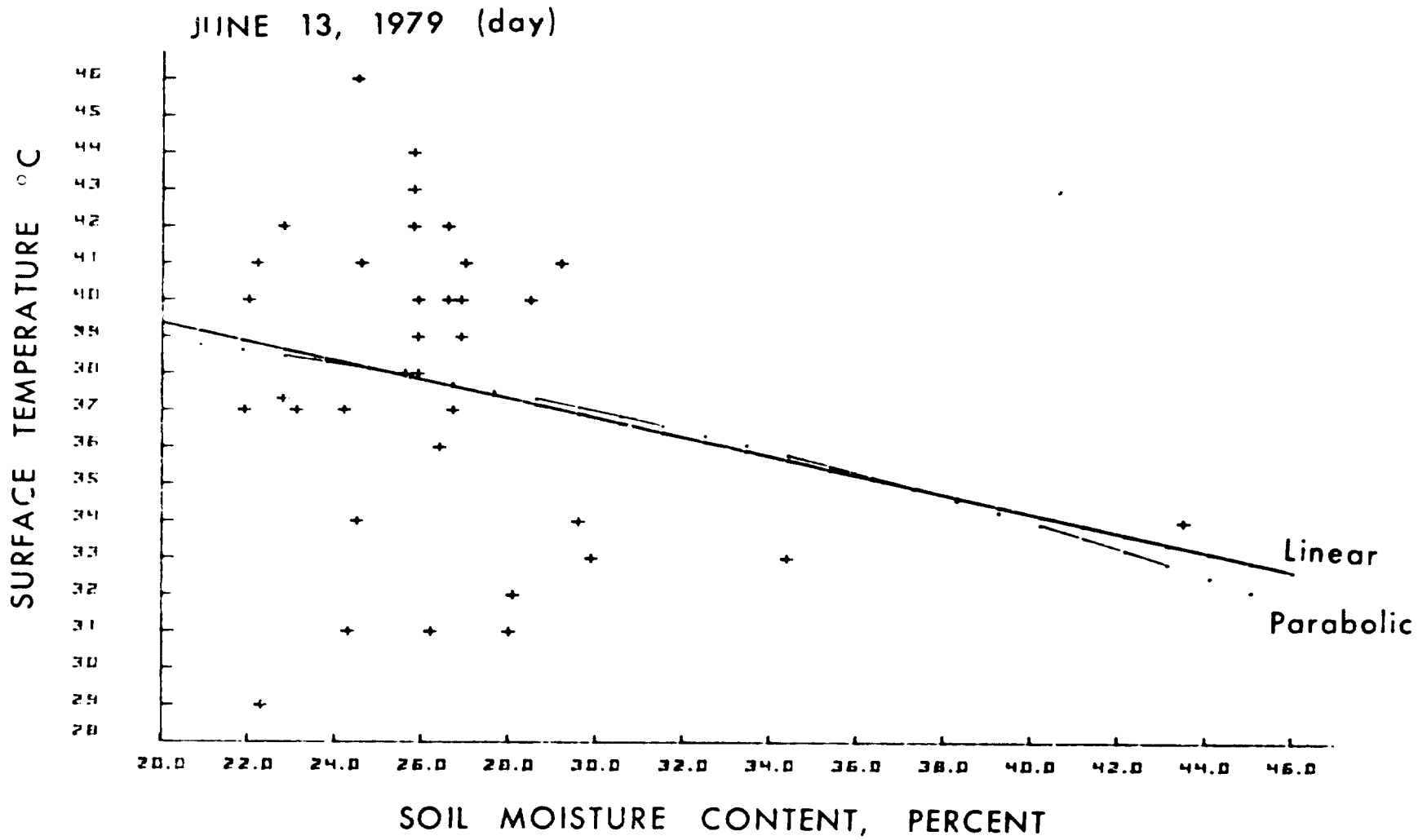

Figure 23. Surface temperature vs. soil moisture content, 6/13/79 data set.

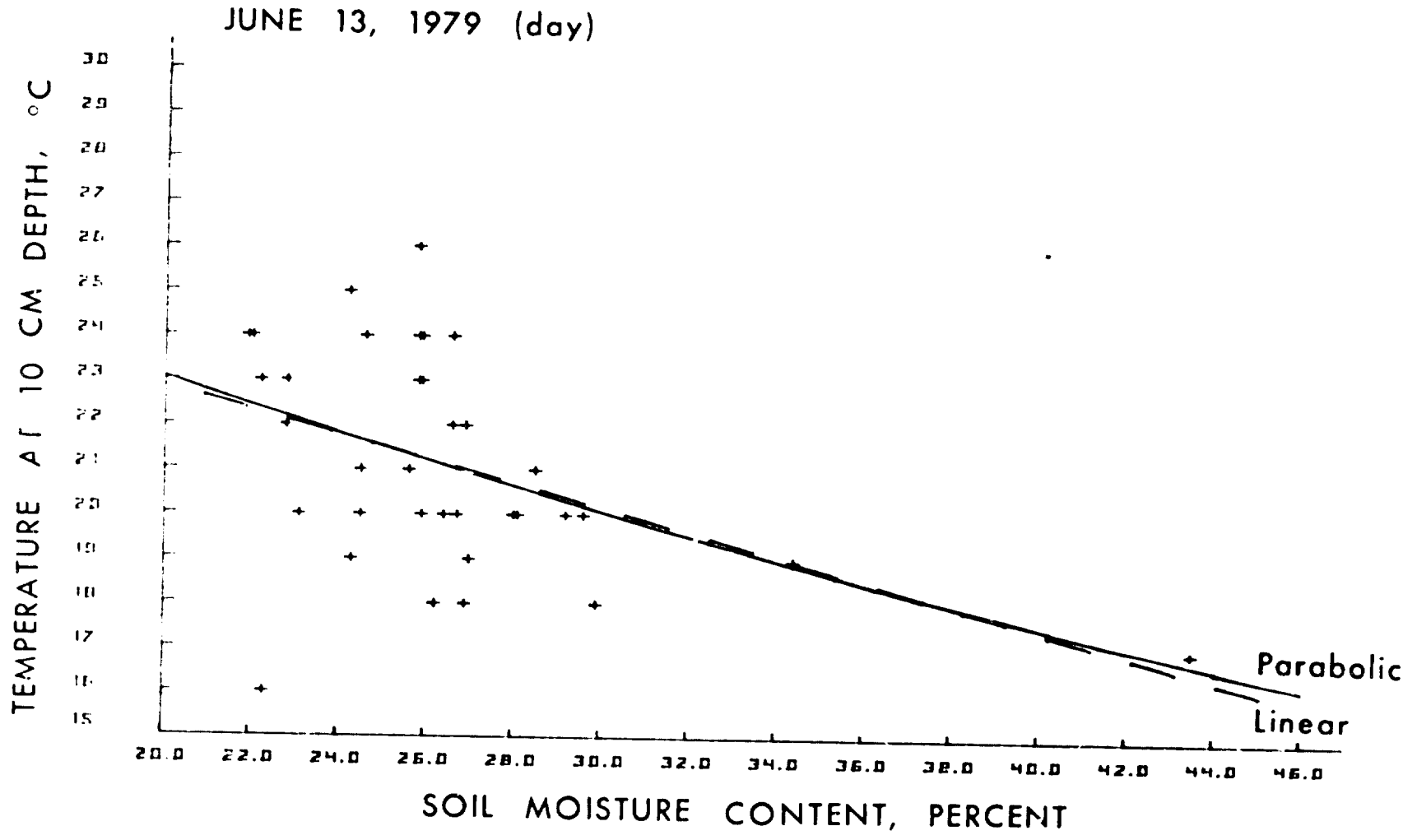

Figure 24. Temperature at 10-cm depth vs. soil moisture content, 6/13/79 data set.

ture data that agreed closely with that obtained from soil samples. Table 3 (Carroll, 1980) compares the two. Flight lines are indicated in Figure 25. The overall root mean square error is 0.9, average bias is -0.3 and percent bias is -1.3. The gamma ray system has been thoroughly tested at the Luverne site since 1970 (Peck, et al., 1980) and the results have a high degree of reliability.

Table 3. Comparison of airborne (gamma ray) derived soil moisture content with ground (soil samples) values, 6/13/79.

Flight Line	Airborne %SM	Airborne Standard Deviation	Ground %SM	Ground Standard Deviation
A	27.5	1.8	27.1	3.5
B	26.1	2.4	25.6	2.3
C	24.5	2.7	24.4	2.6
D	25.3	2.7	26.3	0.5
W	24.9	2.4	26.6	2.3

An unexpected, but well received source of data was that collected by the RS-18-MS flown on the NASA WB57. This flight was not anticipated but resulted from the need for other aircraft missions in the northern plains. Data were collected coincident with the HCMM overpasses of the Luverne test site at 0303 and 1358 CDT on June 13, 1979. Data collected in the predawn flight were limited to the thermal band (10.5-12.5μm). Figure 26 is the portion of the thermal data covering the Luverne flight lines. In the image, warm surfaces appear in light tones; cool surfaces in dark tones. Readily seen in the image are the Rock River, the town of Luverne, Interstate 90 (I-90) and the sewage treatment ponds--all warmer than the surrounding countryside. Thermal differences are also noted in the fields surrounding Luverne, however, the noise pattern, appearing NE to SW across the image contaiminated the data sufficiently that any useful information was lost. This lost information proved to be a real setback when it was impossible to process the nighttime HCMM data, thereby precluding any possible thermal inertial analysis. Thermal data collected during the afternoon suffered from extreme noise contamination

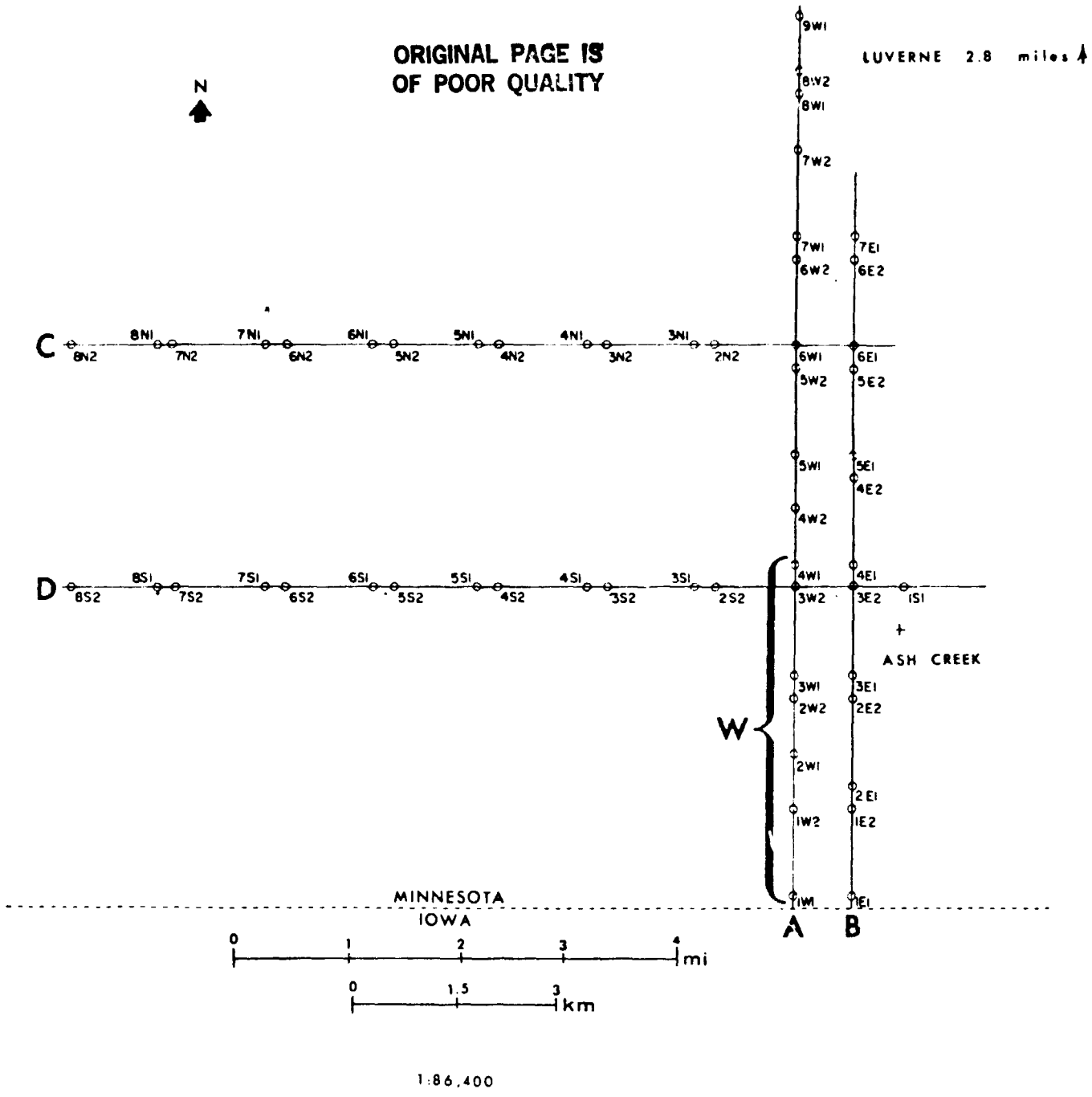

Figure 25. Gamma-ray flight lines at Luverne test site, 6/13/79.

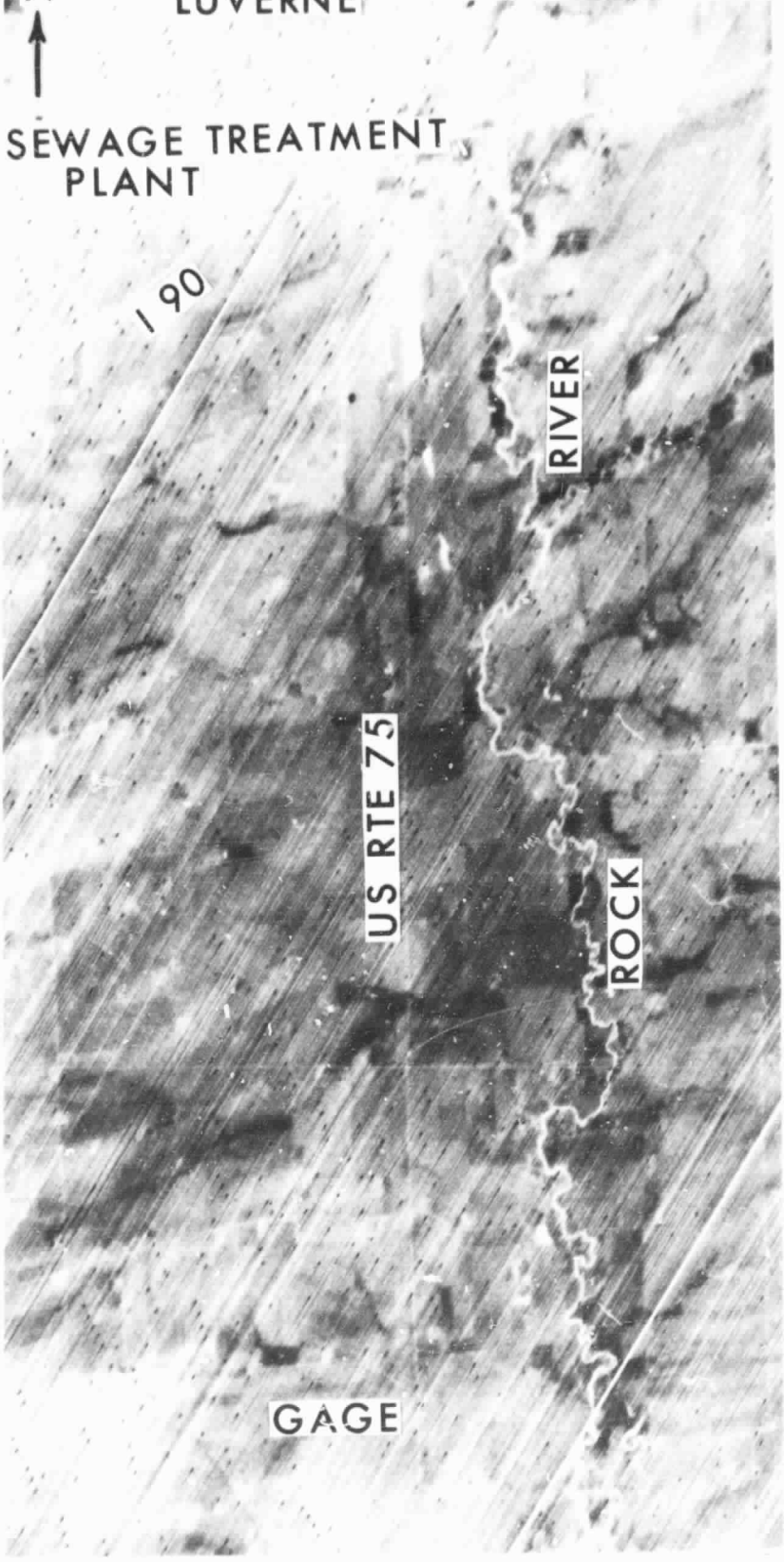

Figure 26. Nighttime (0303 CDT) WB57 HCM thermal-IR image of Luverne test site, 6/13/79, (Approximately 1:90,000).

(see Figure 27). Ironically, visible and false color-IR data (Figures 28 and 29, respectively) were almost noise-free. The experience with NASA-acquired aircraft data taught us that the investigator should contract for such data himself, thereby permitting more flexibility and a greater chance of obtaining useful data.

After a lengthy effort by the HCMM staff at the Goddard Space Flight Center (GSFC), only the daytime HCMM pass could be processed. Figures 30 and 31 are the 1:4,000,000 visible and thermal-IR images respectively, of the 1358 CDT HCMM overpass of the Luverne test site. The area in the immediate vicinity of Luverne is relatively cloud-free, except for a NW to SE band of so-called "invisible cirrus" (because the cloud is not apparent in the visible image) about 25km west of Luverne. The cloud locations are more easily established in the 1:1,000,000 blow-up shown in Figure 32. These images (Figures 30, 31, 32) have been computer processed to enhance the data for best optical contrast. With further enlargement to a scale of approximately 1:360,000 it is possible to overlay the satellite thermal data onto the drainage of the two major rivers in the Luverne vicinity, viz. the Rock River and the Big Sioux River. Figure 33 shows that the land surfaces adjacent to the river systems are cooler than those at higher elevations. This thermal difference is likely due to high water tables and the resultant higher soil moisture content and higher thermal inertia--all of which would contribute to reduced warming during the day (cooler surfaces) and reduced cooling at night (warmer surfaces).

Using digital microfilm printout at full resolution it is possible to compare satellite temperatures (pre-launch calibration) to those measured on the ground during the afternoon of June 13, 1979. The numbers in Figure 34 are in degrees Centigrade. Temperature along the Rock River and its tributaries ranged from 24°C to 29°C. At the same time, temperatures at the higher elevations surrounding the drainage network usually fell between 30°C and 33°C. Comparison

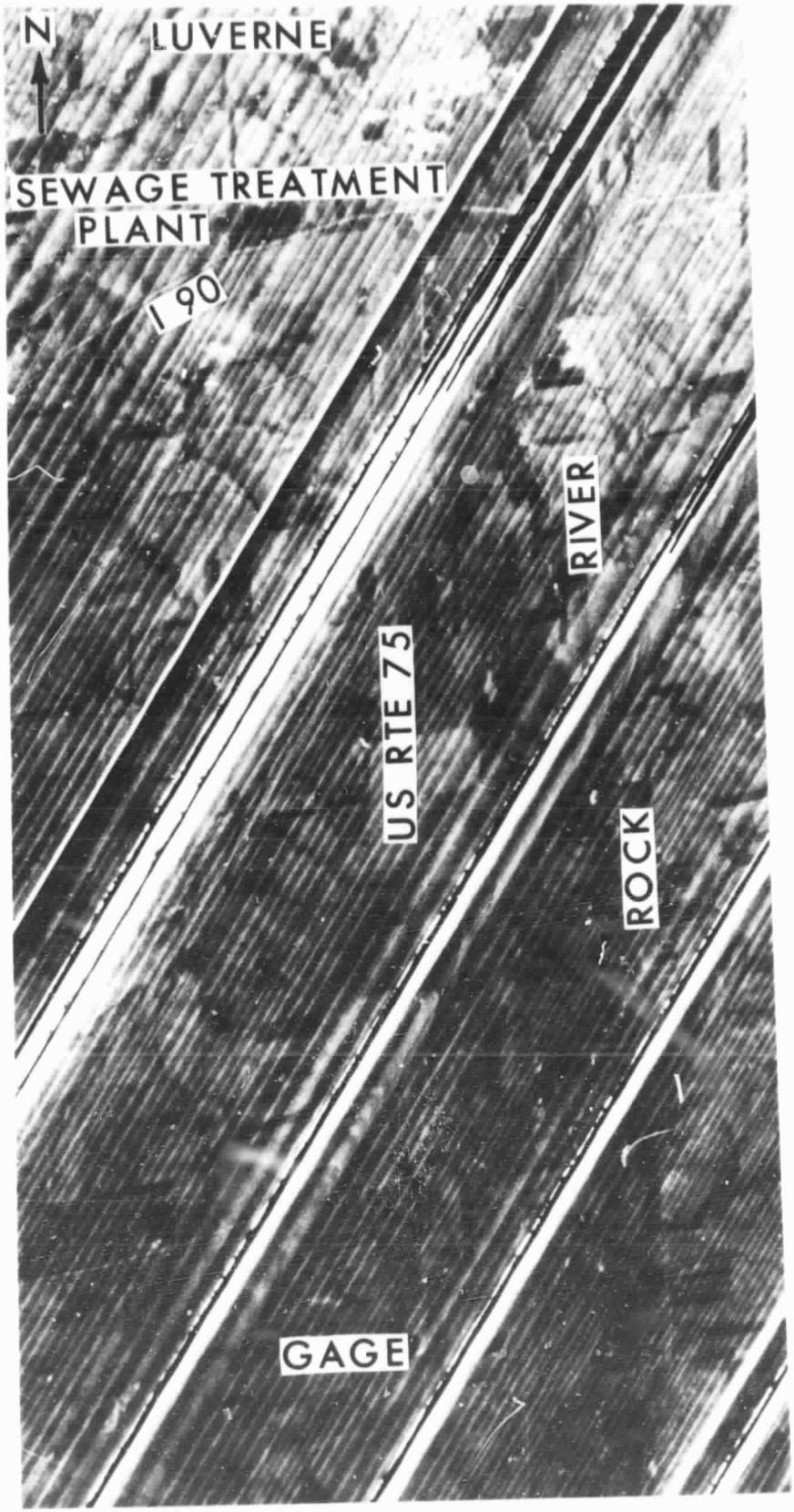

Figure 27. Daytime (1358 CDT) WB57 HCM thermal-IR image of Luverne test site, 6/13/79, (Approximately 1:90,000).

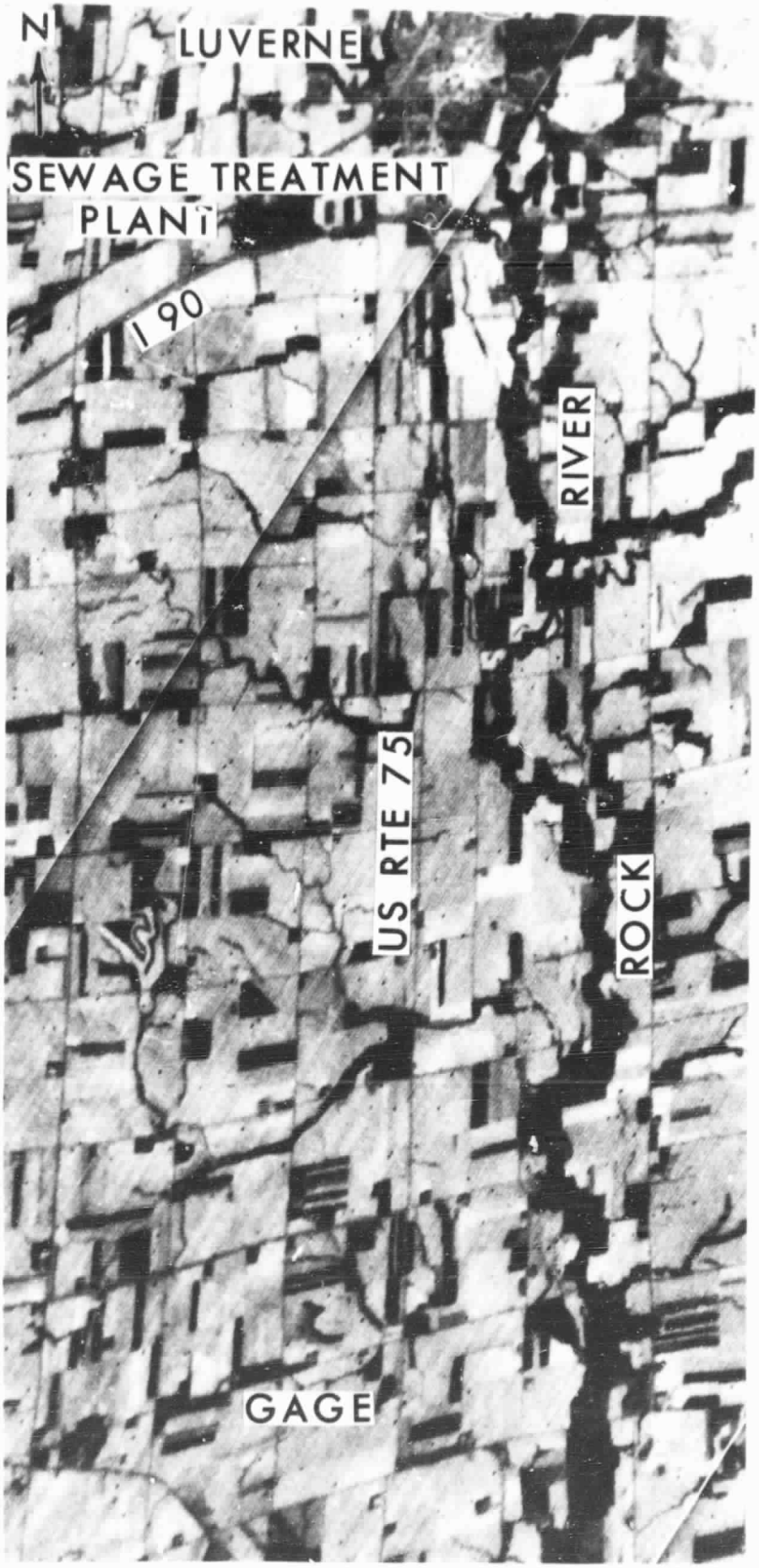

Figure 28. WB57 HCM visible image (1358 CDT) of Luverne test site, 6/13/79. (Approximately 1:90,000).

Figure 29. WB57 Zeiss false color-IR photograph (1358 CDT) of Luverne test site, 6/13/79, (Approximately 1:95,000).

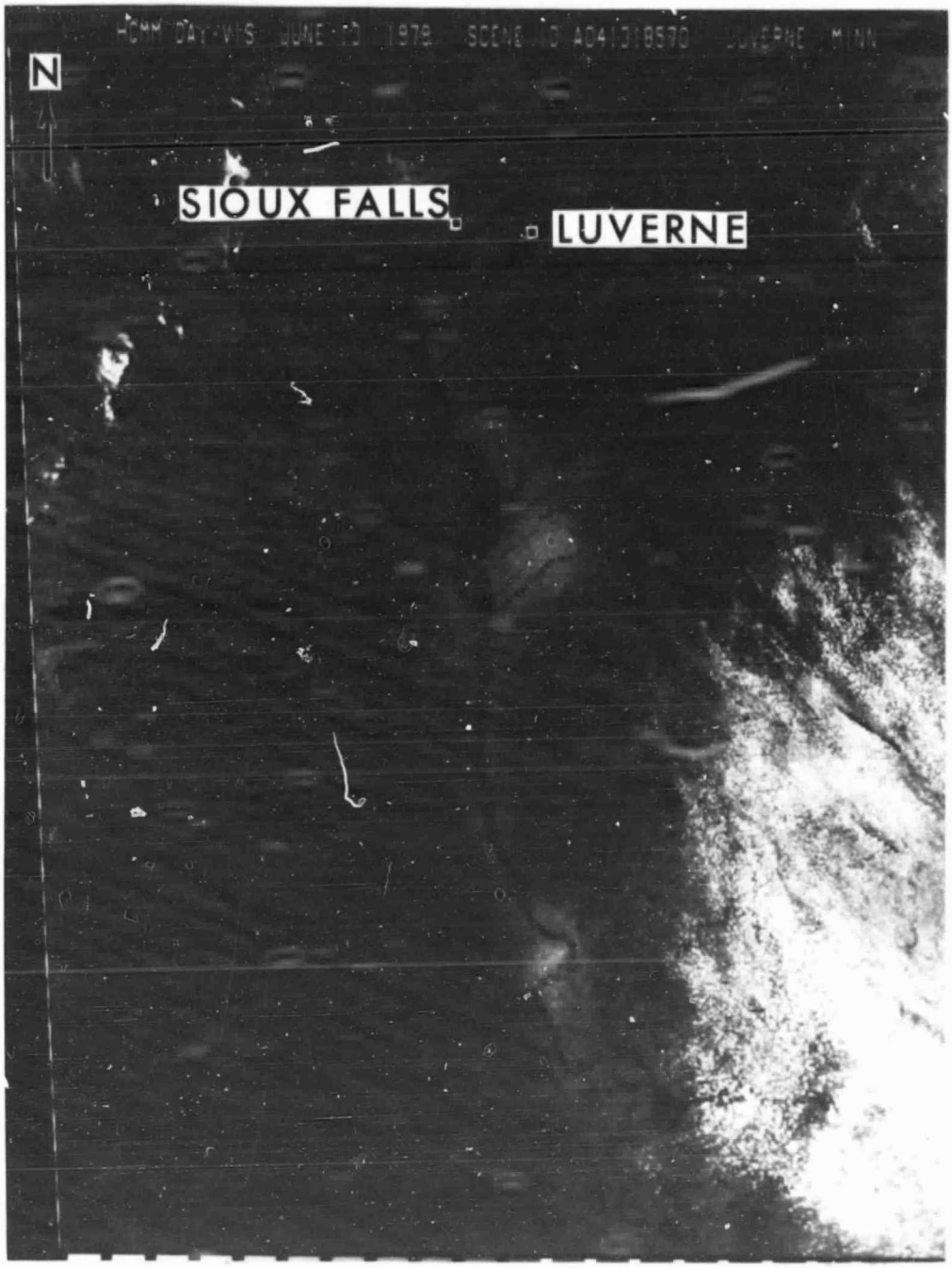

Figure 30. HCMM HCMR visible image (1:4,000,000) of Luverne test site, Scene ID A041318570.

Figure 31. HCMM HCMR thermal-IR image (1:4,000,000) of Luverne test site, Scene A041318570.

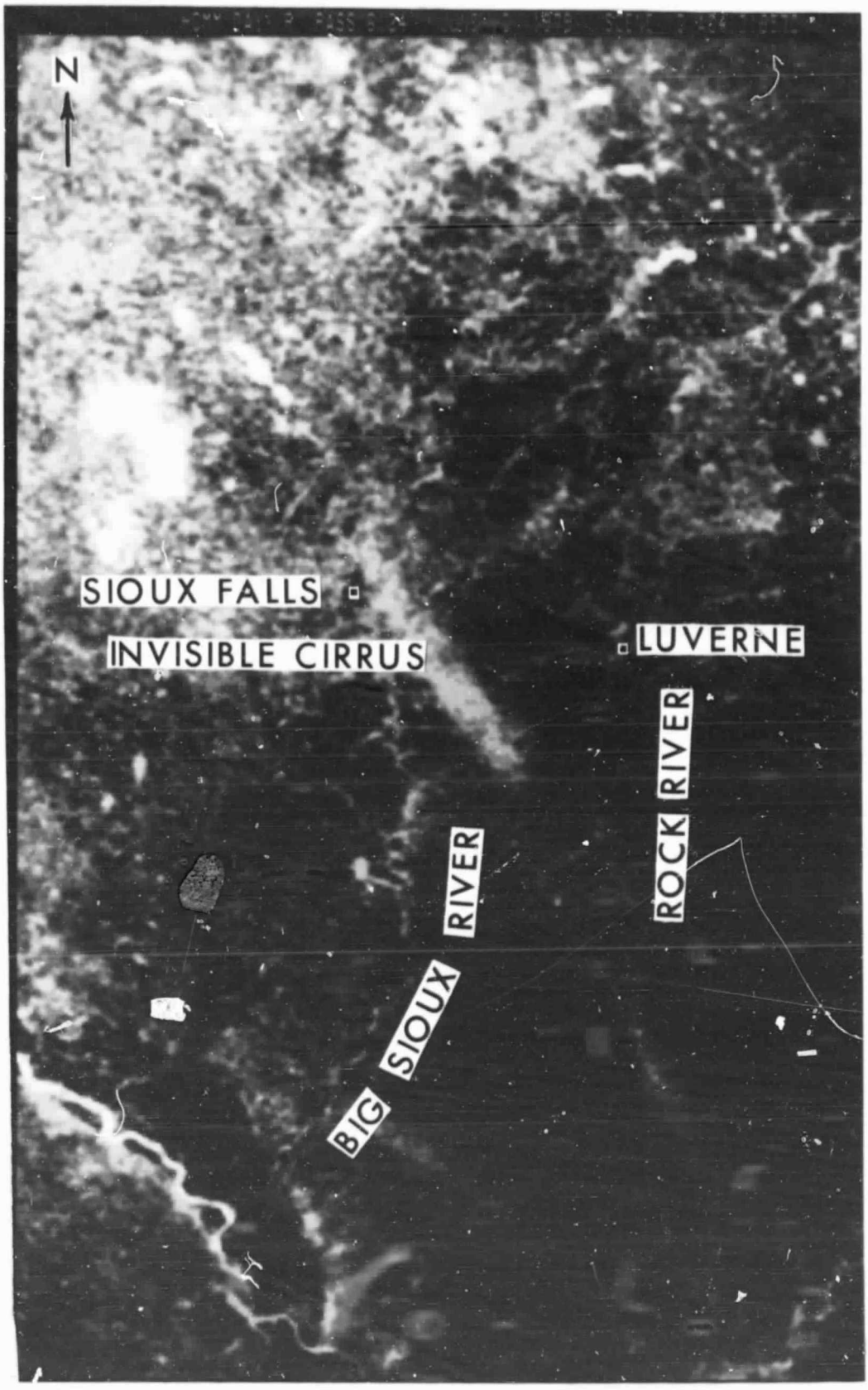

Figure 32. HCMM HCMR thermal-IR image (1:1,000,000) of Luverne test site, Scene ID A041318570.

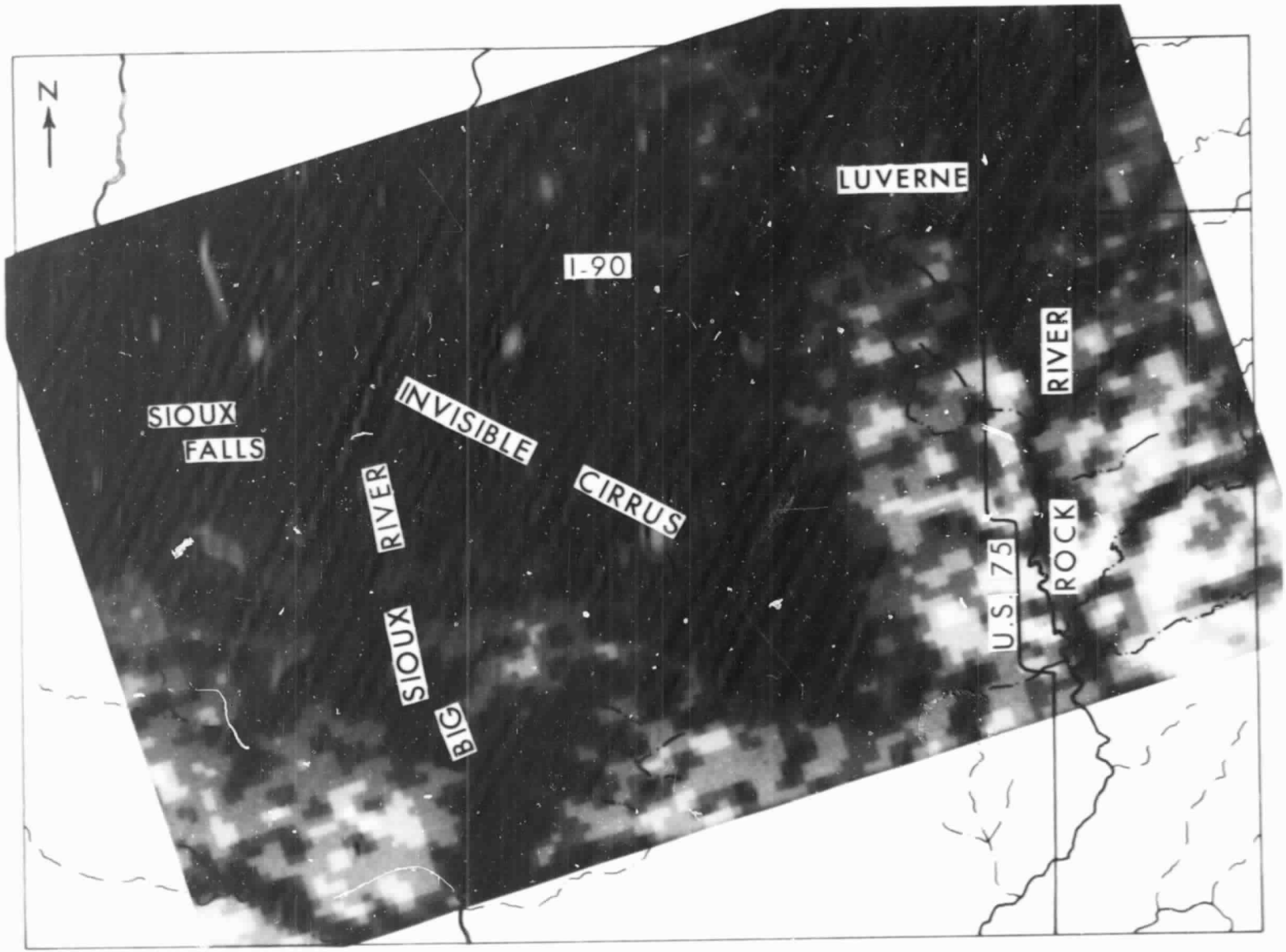

Figure 33. Enlarged HCMM HCMR thermal-IR image (6/13/79) overlaid on drainage network of Luverne vicinity.

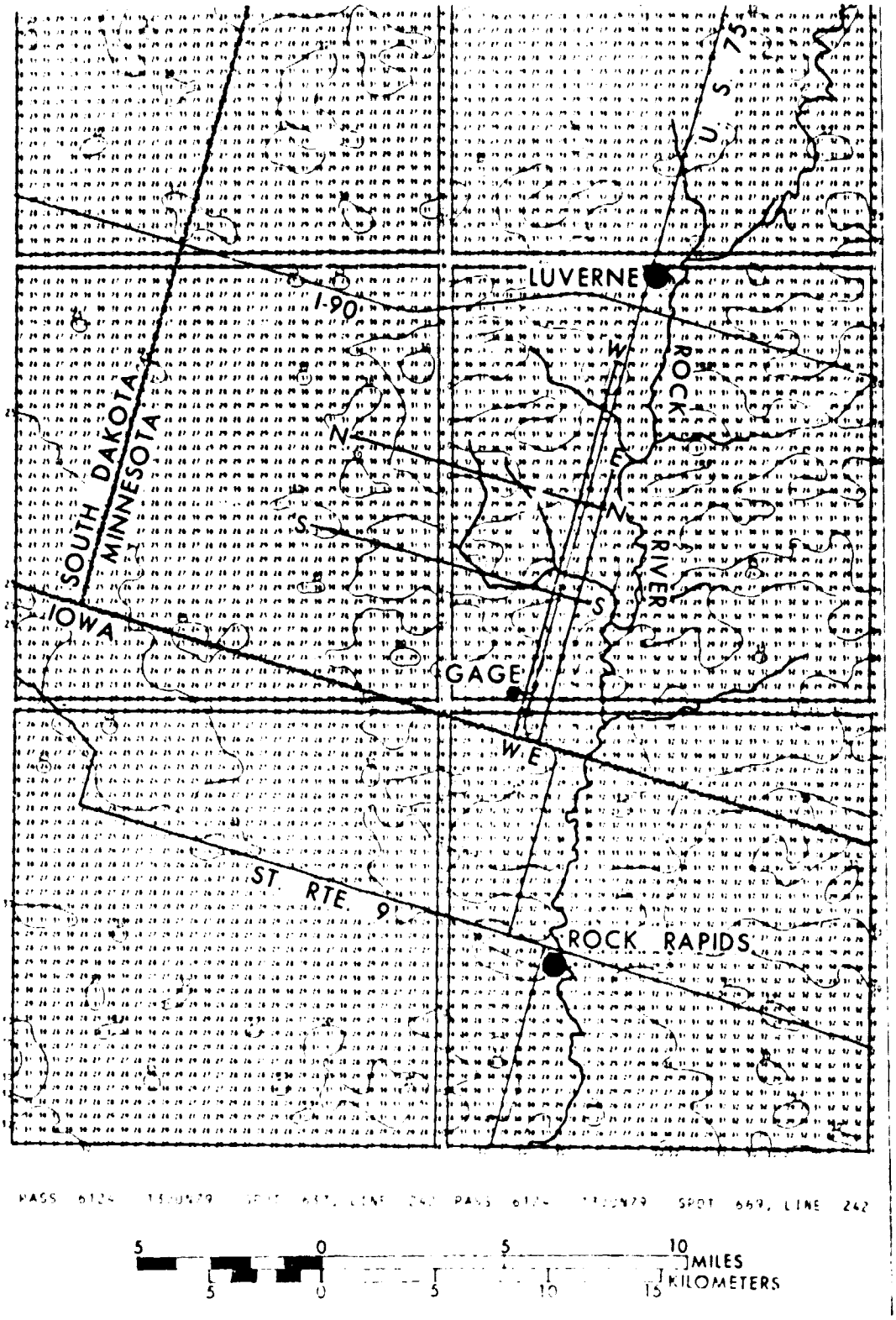

Figure 34. Digital thermal display of HCMM HCMR data (Scene ID A041318570) annotated with drainage network and flight lines of Luverne test site.

with ground-acquired observations showed that HCMR temperatures were consistently 10°C lower than actual surface temperatures. The scale of the data shown in Figure 34 is approximately 1:270,000, indicating that HCMM HCMR data could be easily mapped to conventional scales of 1:250,000 and even 1:125,000--useful scales for many water resource and land use applications.

SUMMARY - SIGNIFICANT RESULTS

Based on the experiences in working with HCMM HCMR data, the following important points must be stressed:

1. Computer programs were developed to enlarge and enhance HCMR data. Imagery may be produced at scales of 1:5,000,000, 1:4,000,000; 1:2,500,000; 1:1,000,000; and 1:500,000. The data are also available in character printout at the same scales as well as 1:250,000.
2. Digital thermal maps (Figure 34) of the Luverne test site were prepared from HCMM tapes.
3. The HCMM thermal inertial approach to soil moisture estimation is unsatisfactory as a NESS operational satellite technique for temperate regions such as Luverne (in the Corn Belt) because of the high incidence of interfering cloud cover. The approach may well be suitable in semiarid regions such as the Southwest.
4. The thermal-inertia technique for estimating soil moisture as exemplified by the HCMM experiment is unsatisfactory, as an operational system due to frequent cloud cover as well as difficulties in processing the data. If NESS were to require a soil-moisture sensor, we would recommend an all-weather system such as passive or active microwave.

REFERENCES

Batlivala, P.P. and Ulaby, F.T., 1977, "Feasibility of Monitoring Soil Moisture Using Active Microwave Remote Sensing," The Univ. of Kansas Center for Research, Inc., RSL Technical Report 264-12, NASA/JSC Contract NAS 9-14052.

Blanchard, M.B., Greeley, R., and Goettelman, R., 1974, "Use of Visible, Near-Infrared and Thermal Infrared Remote Sensing to Study Soil Moisture," NASA TM X-62, 343, 8 pp.

Carroll, T.R., 1980, personal communication.

Feimster, E.L., Fritzsche, A.E., and Jupiter, C., 1975, "Soil Moisture Survey Experiment at Phoenix, Arizona," EG&G Report No. 1, EGG-1183-1674, Las Vegas, Nev., 30 pp.

Fuchs, M. and Tanner, C.G., 1968, "Surface Temperature Measurements of Bare Soils," J. Applied Meteorology, Vol. 7, pp. 303-305.

Gillespie, A.R. and Kahle, A.G., 1977, "Construction and Interpretation of a Digital Thermal Inertia Image," Photogrammetric Engineering and Remote Sensing, Vol. 43, No. 8, pp. 983-1000.

Idso, S.G., Schmugge, T.J., Jackson, R.D., and Reginato, R.J., 1975, "The Utility of Surface Temperature Measurements for the Remote Sensing of Surface Soil Water Status," Journal of Geophysical Research, Vol. 80, No. 21, pp. 3044-3049.

Jackson, R.D., Reginato, R.J., and Idso, S.B., 1975, "Timing of Ground Truth Acquisition during Remote Assessment of Soil-Water Content," Remote Sensing of Environment, Vol. 6, No. 4, pp. 249-255.

Merritt, E.S. and Hall, C., 1973, Soil Moisture Estimation Applications of Nimbus-3 HRIR-D (0.7-1.3μm) Observations, Final Report, Earth Satellite Corp., Contract No. 2-37098, 45 pp.

Peck, E.L., Bissell, V.C., Jones, E.B., and Burge, D.L., 1971, "Evaluation of Snow Water Equivalent by Airborne Measurement of Passive Terrestrial Gamma Radiation," Water Resources Research, Vol. 7, No. 5, pp. 1151-1159.

Peck, E.L., Carroll, T.R., and Vandemark, S.C., 1980, "Operational Aerial Snow Surveys in the United States," Hydrologic Sciences Bulletin, Vol. 25, No. 1, pp. 51-62.

Schmugge, T., 1976a, "Preliminary Results from the March, 1975 Soil Moisture Flight," NASA/Technical Memorandum, TMX 73197, 16 pp.

Schmugge, T., 1976b, "Remote Sensing of Soil Moisture," NASA X-913-76-118.

Schmugge, T., Blanchard, B., Burke, W., Paris, J., Wang, J., 1976, "Results of 1974 Soil Moisture Flight," NASA TM C-8193, Wash., D.C., 58 pp.

Schmugge, T.J., Jackson, T.J., and McKim, H.L., 1980, "Survey of Methods for Soil Moisture Determination," Water Resources Research, Vol. 16, No. 6, pp. 961-979.

Schmugge, T., Wilheit, T., Webster, Gloersen, P., 1976, "Remote Sensing of Soil Moisture with Microwave Radiometers-II," NASA TN D-8321, Wash., D.C., 34 pp.

Wang, J.R., Shiue, J.C., and McMurtrey, J.E., 1980, "Microwave Remote Sensing of Soil Moisture Content over Bare and Vegetative Fields," Geophysical Research Letters, Vol. 7, No. 10, pp. 801-804.

Wiesnet, D.R., McGinnis, D.F., Matson, M., 1978, "Selected Hydrologic Applications of Landsat-2 Data: An Evaluation," Final Report to NASA/GSFC, Contract No. NAS-53991A.

PART C: A COMPARISON OF HCMR AND AVHRR IMAGES OF URBAN HEAT ISLANDS

On the night of March 16-17, 1979, both HCMM and NOAA-6 thermal-IR (10.5-11.5μm) imagery were taken over the Washington, D.C. and Baltimore, Md. area. The NOAA-6 image (Figure 35) was taken on the evening of March 16 at 2000 EST and the HCMM image (Figure 36) was taken 6 hours later at 0200 EST in the early morning of March 17. Both images were computer enlarged to 1:1,000,000. Although each satellite has a different resolution (1.1km for NOAA-6 and 0.6km for HCMM), the urban heat island structure of Washington, D.C. and Baltimore are remarkably similar in both images. In each the warmest (darkest) urban areas run southwest-north-east in Washington, D.C. and southeast-northwest in Baltimore. On the NOAA-6 image the highest satellite-measured temperatures for the D.C. area range from 12.4 -13.4°C and for Baltimore from 14.0-15.5°C. Six hours later the highest HCMM brightness temperatures were 6.0-8.0°C for Washington, D.C. and 8.0-12.0°C for Baltimore. The cooling over this six-hour period, however, may not be as great as indicated because of calibration problems with the HCMM data. Pre-flight calibration was used to generate the brightness temperatures used here.

Temperatures outside the warmest urban areas ranged from 9.7-11.9°C on the NOAA-6 image and from 4.0-6.0°C on the HCMM image. Several industrial and suburban areas can also be identified on each image: (1) Sparrows Point steel plant, (2) Glen Burnie, Md., (3) Laurel, Md., (4) Fort Meade, Md, (5) Bowie, Md., (6) Springfield, Va., and (7) Manassas, Va.

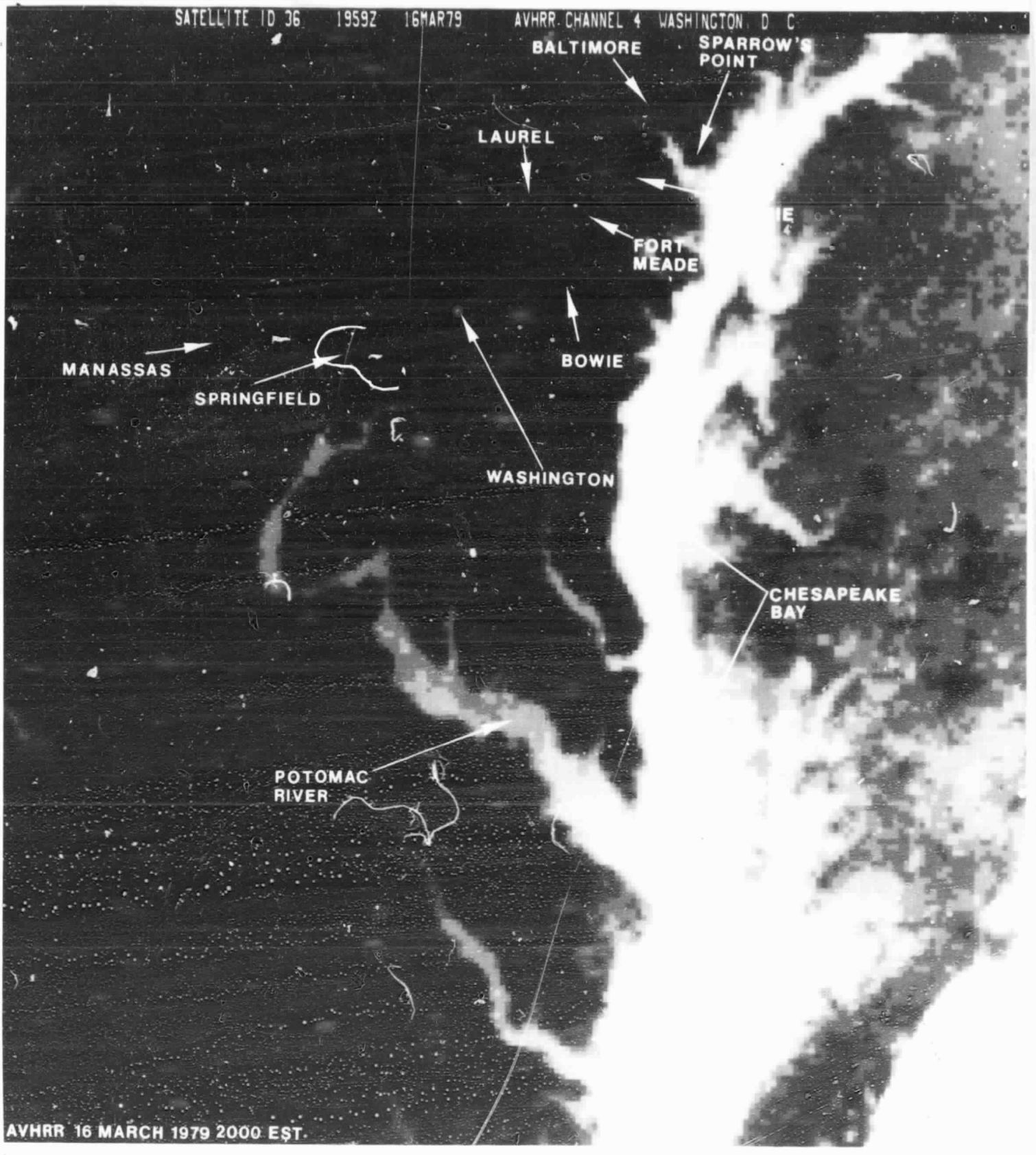

Figure 35. NOAA-6 11μm AVHRR image of the Washington, D.C. and Baltimore area taken on March 16, 1979, at 1959 GMT. The warmer urban and suburban areas show up as dark gray shades. Resolution is 1.1 km.

Figure 35. NOAA-6 11μm AVHRR image of the Washington, D.C. and Baltimore area taken on March 16, 1979, at 1959 GMT. The warmer urban and suburban areas show up as dark gray shades. Resolution is 1.1 km.

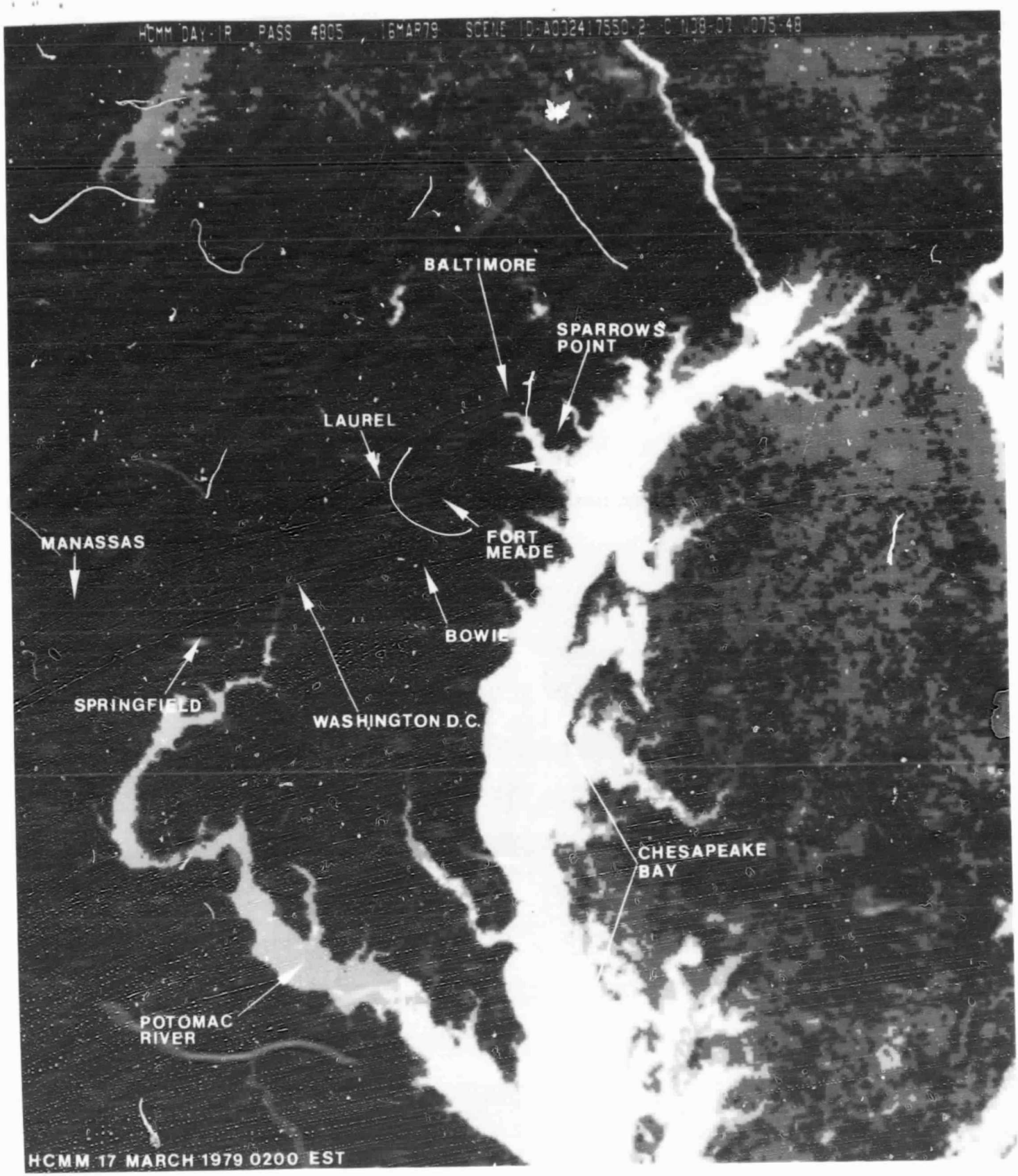

Figure 36. HCMM 11μm image of the Washington, D.C. and Baltimore area taken on March 16, 1979, at 0100 GMT. The warmer urban and suburban areas show up as dark gray shades. Resolution is 0.5 km.

APPENDIX A

HEAT CAPACITY MAPPING MISSION (HCMM) THERMAL SURFACE WATER MAPPING OF LAKE ANNA, VA. AND ITS CORRELATION TO LANDSAT

United States Department of the Interior

GEOLOGICAL SURVEY
RESTON, VA. 22092
National Center, MS 522

March 3, 1980

Memorandum for the Record (EC-74-Landsat)

By: EROS Coordinator, National Mapping Division

Subject: Heat Capacity Mapping Mission (HCMM) thermal surface water mapping and its correlation to Landsat

The Heat Capacity Mapping Mission (HCMM) involves a relatively simple satellite recording the radiation from the Earth in the thermal band (10.5 to 12.5 μm) using an instantaneous field-of-view (IFOV, "footprint" or pixel) of 600 x 600 m. The enclosed graphics illustrate HCMM thermal mapping of water bodies as applied to Lake Anna. The HCMM digital data were produced by NASA and processed by the National Oceanographic and Atmospheric Administration/National Environmental Satellite Service (NOAA/NESS) into image and line-printer form for the U.S. Geological Survey. A Landsat image of Lake Anna illustrates the relationship between the Landsat multispectral scanner (MSS) and the HCMM data as now processed by NASA through their Image Processing Facility (IPF) which transforms the data to the same distortion-free Hotine Oblique Mercator (HOM) map projection. Spatial correlation of the two images is relatively simple by either analog or digital means and the HCMM image has a potential accuracy (root-mean-square error--rmse) approaching the 80 m of the original Landsat data.

Lake Anna was built and filled during 1968-72 to provide cooling for a nuclear power plant. The lake covers about 5,300 hectares (13,000 acres), but because of its dendritic shape, it is hard to find open reaches of more than 2 or 3 km. Approximately 1,200 hectares (3,000 acres) comprise the actual cooling ponds for the nuclear reactors, and they again are broken into odd shapes with open reaches generally limited to 1 or 2 km. The HCMM IFOV is a nominal 600 x 600 m, and the data have been resampled by cubic convolution which alters original IFOV response both geometrically and radiometrically. Thus it is difficult to get a thermal reading of the cooling ponds which has not been diluted by radiation from the considerably cooler adjacent land areas.

On the figure that displays both image and line-printer HCMM data, the image form fails to display the subtle temperature differences because of the range and contrast used in the reproduction process. However, the digital data as indicated by the line printer displays five different temperatures, all of which represent open-water areas. Again, the narrow portions of the lake fail to show suitable readings because the land area dilutes the response of the 600- x 600-m footprints near the shoreline.

On June 11, 1978, when the HCMM data were obtained, thermometers were recording temperatures (surface, mid- and bottom depths) at no fewer than nine locations distributed throughout the lake. The thermometer readings clearly indicated that the pre-launch HCMM calibration data could not be applied directly to Lake Anna readings. Where thermometers indicated surface temperatures of 23.7° C, the HCMM reading based on pre-launch calibration recorded 14.3° C. Thus, 9.4° C were added to the pre-launch-based values. The resulting correlation indicates that, where the water-surface response was not diluted by land areas, the temperature difference recorded by the HCMM correspond to the in situ temperature readings with rmse on the order of 1° C. Thus, the temperature gradients in the larger areas of cooling ponds and main lake body are recorded in useable and relatively accurate form.

Other sites of known surface-water temperature must be tested before conclusions can be reached as to the areal and temporal frequency of calibration needed to effectively map water-surface temperature with HCMM data. Moreover, the atmosphere and surface conditions under which such thermal sensing is or is not practical remain to be defined. It is considered significant that a satellite with as coarse a footprint as the HCMM can provide meaningful data of a water body as small and irregular as Lake Anna and that the data can be spatially correlated with other data sets such as those of Landsat.

Alden P. Colvocoresses

Enclosures 2

CORRELATION OF HCMM AND LANDSAT DATA LAKE ANNA, VA.

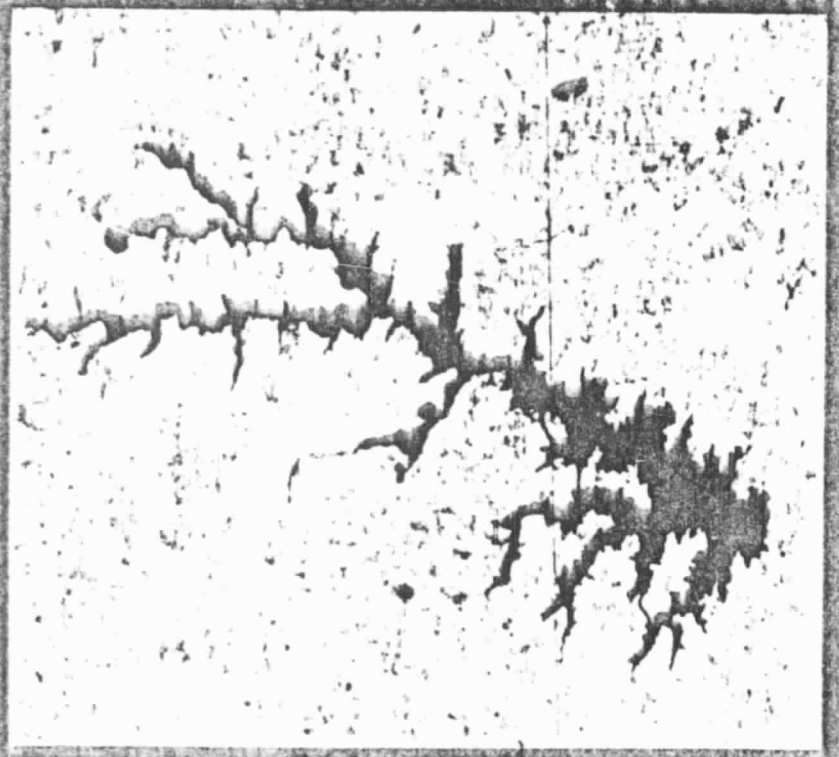

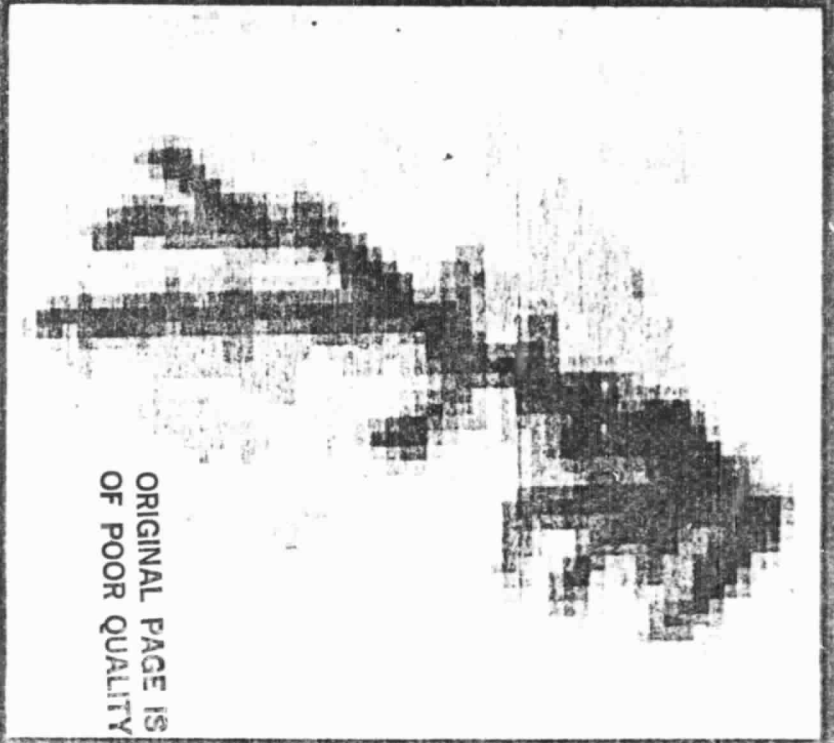

ORIGINAL PAGE IS OF POOR QUALITY

LANDSAT MSS BAND 7
JULY 8, 1973
80 X 57M PIXEL

HCMM*
JUNE 11, 1978 NIGHT
600 X 600M PIXEL

5 0 5 10 15 20 KILOMETERS

*HCMM data furnished by NOAA/NESS

HCMM THERMAL MAPPING OF LAKE ANNA, VA.

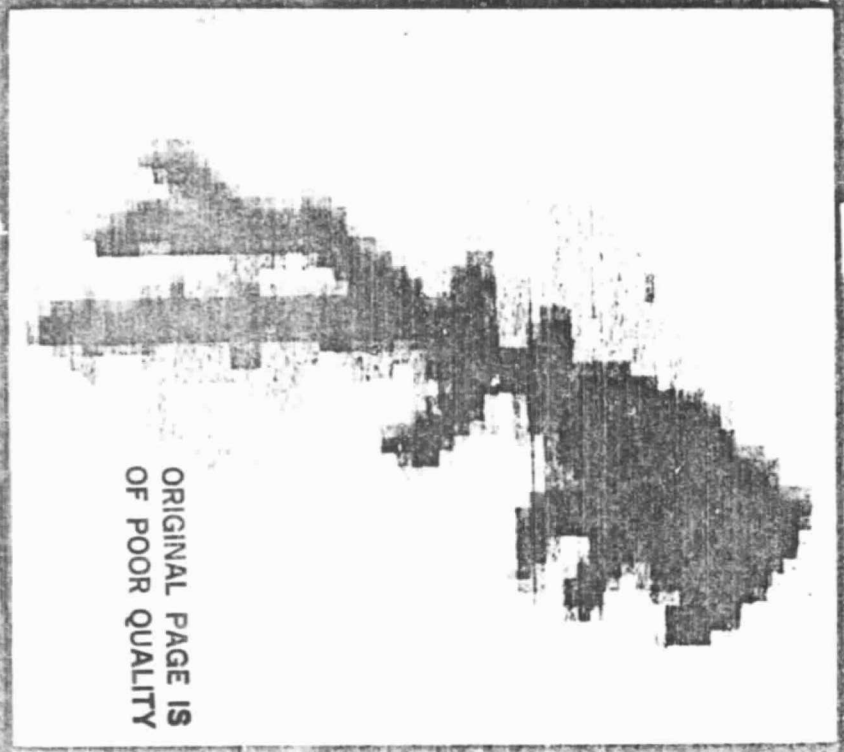

ORIGINAL PAGE IS
OF POOR QUALITY

IMAGE FORM

LINE PRINTER PLOT

5 0 5 10 15 20 KILOMETERS

Time and Date of Imagery, 03:29 EDST, June 11, 1978